NTNU
Norwegian University of
Science and Technology

Two Dimensional Fiber Bundle Bridge Model

Håkon Tormodsen Nygård

Master of Science in Physics and Mathematics
Submission date: June 2016
Supervisor: Alex Hansen, IFY

Norwegian University of Science and Technology
Department of Physics

Abstract

The two dimensional fiber bundle bridge model is introduced, derived and studied for an uniform threshold distribution. The model is independent of history and has an adjustable effective range of interaction, which is adjusted by the effective spring constant β. For high values of β the systems are soft and for low values the systems are stiff.

In the limit of stiff systems the model is shown to be equivalent to the equal load sharing model, which is supported by the results for the strain curve, average size of largest cluster S_{MAX}, average number of clusters N_d, average distance between two consecutively breaking fibers $\langle \Delta r^2 \rangle^{1/2}$ and burst size distribution $D(\Delta)$. The model is not equivalent to the local load sharing model for soft systems, the behaviour is closer to the behaviour of the soft clamp model for soft systems. For soft systems a circularly shaped cluster of broken fibers develops for both models when sufficiently many fibers are broken. After the cluster has formed, the fibers breaking are close to or in its perimeter, expanding the size of the circular cluster. The bridge model represents a very thin bendable plate with holes, while the soft clamp model represents an infinitely thick elastic plate. It is therefore expected to be some differences between the models, but the amount of comparable data at the time of writing is unfortunately insufficient to pinpoint clear differences.

Sammendrag

Den todimensjonale fiberbuntbromodellen blir introdusert, utledet og studert for en uniform terskelfordeling. Modellen er historieuavhengig og har en justerbar effektiv rekkevidde for vekselvirkningene, som justeres av den effektive fjærkonstanten β. Systemet er mykt for høye verdier av β og stivt for lave verdier.

I grensen av stive systemer er modellen vist å være ekvivalent med the demokratiske lastdelingsmodellen, noe som støttes av resultatene for lastkurven, gjennomsnittlig størrelse av den største klyngen av brukne fiber S_{MAX}, gjennomsnittlig antall klynger av brukne fiber N_d, gjennomsnittlig distanse mellom fiber som brekker etter hverandre $\langle \Delta r^2 \rangle^{1/2}$ og glippfordelingen $D(\Delta)$. Modellen er ikke ekvivalent med den lokale lastdelingsmodellen for myke systemer, oppførselen er nærmere oppførselen til "soft clamp"-modellen for myke systemer. For myke systemer utvikler det seg en sirkulær klynge av brukne fiber når mange nok fiber er brukket. Etter at klyngen er blitt dannet er fiberene som ryker nære eller i perimeteren til klyngen, som ekspanderer størrelsen til den sirkulære klyngen. Bromodellen representerer en veldig tynn bøyelig plate med hull i, mens "soft clamp"-modellen representerer en uendelig tykk elastisk plate. Det er derfor forventet at det er noen ulikheter mellom modellene, men mengden av sammenlignbare data er dessverre utilstrekkelig på nåværende tidspunkt til å fastlå klare ulikheter.

Preface

This thesis concludes my work for the degree of Master of Science in Applied Physics at the Norwegian University of Science and Technology (NTNU), and corresponds to 30 ECTS credits. It introduces the two dimensional fiber bundle bridge model, which is based on the one dimensional bridge model developed in my specialization project in physics at the Department of Physics at NTNU. Both this thesis and the specialization project has been performed under the supervision of Prof. Alex Hansen at the Department of Physics at NTNU. Since this thesis is based on my specialization project, which is unpublished, the derivation of the one dimensional model is included in this text to give a complete derivation of the two dimensional model.

There are several persons I would like to thank for helping me along the way during the project and supporting what I do. First I would like to thank Prof. Alex Hansen for providing this fascinating project and his continued guidance and support during the the whole process. I have thoroughly enjoyed working together with all the members of the fiber bundle model research group, which includes master students Eivind Bering, Magnus H.-S. Dahle and Jørgen Vågan and the Ph.D. students Jonas T. Kjellstadli and Morten Vassvik. Their advice and support has helped keeping the project on track and sharing knowledge has sped up the progress. I would also like to give a special mention to the regular lunch group I have been part of for taking my mind off fiber bundle models for some time each day. Last, but not least, I would like to thank my family for the continued great moral support, with a special mention to my brother Øystein who has given me inputs and feedback throughout the process.

Trondheim, June 15, 2016

Håkon Tormodsen Nygård

Contents

List of Figures

1 Introduction

Fracture and materials failing is something most humans have experience with since it is fairly common occurence. Wether it is a bone in the body breaking, buildings or other constructions failing or something as simple as pulling to objects glued together apart. Simulating fracture of materials accurately with all effects present in the model is exceedingly difficult, which is why methods using approximations are used. Fiber bundle models are one of these approximated methods, and the materials are represented by a bundle of elastic fibers which fail if they are extended too far.

The first fiber bundle model was introduced by Peirce in 1926 [1] in an attempt to study the strength of cotton yarns. Computers were not available at the time and the model reflects this by having a mean field behaviour, which enabled him to look at analytical results in his quest to study the strenght of cotton yarns. It would take more than 50 years before the local load sharing model was introduced by Harlow and Phoenix in [2], which is the extreme opposite of the equal load sharing model. The model was introduced as a more realistic model for composite materials, and it distributes the force previously carried by failed fibers to the nearest intact fibers only. The models is far harder to get analytical results for, but the computer had already been introduced to the world before 1978. Both models are very well suited to be simulated on computers in order to get average results and reveal the behaviour of the models.

The equal load sharing model was introduced to look at cotton yarns and the local load sharing model to look at composite materials, but this is far from the only application of fiber bundle models. The fibers do not necessarily have to be fiber, it only needs to have a threshold value which can not be exceeded without breaking it. One example of creative use of fiber bundle models are Pollen et al. using a fiber bundle model approach to estimate the effects of riparian growth on the stability of stream banks in [3]. Two other examples of creative use of fiber bundle models are to look at snow avalanches, which was done in [4], and to look at at traffic jams, done in [5].

Neither the equal or the local load sharing models are the most realistic models of materials. A model between these two extreme models is the soft clamp model by Batrouni et al. [6] where two infinite half-planes of elastic material are glued together by elastic fibers. With this model it is possible to change the stiffness of the elastic half-planes connected together, thus changing the effective range of interaction in the model.

Inspired by the approach in the soft clamp model, the one dimensional bridge model consisting of a bendable cable causing the change in force in the system was introduced in [7] by this author. The goal in this thesis is to develop the model in two dimensions based

on the one dimensional model, which was shown to have an adjustable effective range of interaction in [7]. When the model has been derived we want to produce selected results and try to give a qualitative description of the quantitative results. Where natural and possible we also want to compare the model to existing models like the equal and local load sharing model and the soft clamp model. In short form we want to:

- Derive and introduce a two dimensional model based on the one dimensional bridge model.
- Produce selected results and try to give them a qualitative description.
- Compare the results to established models when both natural and possible.

This document is divided in six different chapters, where this chapter is chapter 1. The models are presented in chapter 2 and the methods used to simulate the models and algorithms are presented in 3. The results are found in chapter 4 and later discussed in chapter 5, and the conclusion and suggestions for future work are in chapter 6.

2 Fiber Bundle Models

The first fiber bundle model was introduced in 1926 by Peirce [1] to study the strength of cotton yarns. The model distributes the total force equally between all intact fibers, and is known as the equal load sharing fiber bundle model. Since its introduction several new, more advanced models have been introduced, like the local load sharing model by Harlow and Phoenix [2].

Section 2.1 describes some of the general properties of fiber bundle models, and the equal load sharing model is outlined in section 2.2. The one dimensional fiber bundle bridge model, originally presented in [7] by this autor, is described and derived in section 2.4. Since [7] is unpublished, the derivation and description of the model is included here in a slightly rewritten form. The two dimensional bridge model, based on the one dimensional model, is introduced and derived in section 2.5.

2.1 General Properties

Fiber bundle models seek to describe the failure process for a bundle of fibers. For the models described here all fibers have a finite threshold extension, and a fiber breaks irreversibly if it is extended beyond its treshold. Periodic boundary conditions in all directions are used for all the models ensuring all fibers have the same number of neighbours and can all be treated equally.

2.1.1 Threshold Distribution

A fiber bundle is a system of N fibers which are modelled as ideal, elastic springs following Hooke's law

$$f(\chi) = \kappa\chi, \tag{2.1}$$

where κ is the spring constant and χ is the extension of the fiber in question. All fibers have a given threshold extension, denoted $\chi_{i,j}$ for two dimensional models. The threshold extension is drawn from a chosen probability distribution, known as the threshold distribution. The threshold distribution will be represented by its cumulative distribution function

$$P(\chi) = \text{Prob}\left(\chi_{i,j} \leq \chi\right), \tag{2.2}$$

where $P(\chi)$ is always in the interval between zero and one.

The threshold distribution used here will be the uniform distribution between 0 and χ_r, which is given by the cumulative distribution function

$$P(\chi) = \begin{cases} \dfrac{\chi}{\chi_r} & \text{for } \chi < \chi_r \\ 1 & \text{for } \chi \geq \chi_r \end{cases}. \tag{2.3}$$

Henceforth, the threshold distribution in (2.3) will simply be denoted $P(\chi) = \chi/\chi_r$. All cumulative distribution functions have a minimum value of 0 and a maximum value of 1, making the extra information in (2.3) redundant. The statistically uniform distribution in (2.3) is widely used as the average properties are identical to the average properties of the strictly uniform distribution for large system sizes N [8]. If N fibers have strictly uniformly distributed threshold values, the difference in numerical value between the weakest and second weakest fiber is the same as the difference between the second and third weakest and so on. Using this property many analytical results can be derived, but it is not well suited to simulations due to always giving the same values. Hence the threshold values are statistically uniformly distributed. Most results are averages of many realisations, and the average properties is the same for both distributions.

2.1.2 Strain Curve

There are two different methods for loading the system of fibers. One possibility is to increase the total force on the system in finite increments. Such loading of the system may result in zero, one or several fibers breaking for each increment of the total force. When the system reaches the critical total force, all remaining intact fibers break simultaneously. Using the incremental loading of the system results in no information about the minimum force required to break the fibers after the critical force has been reached. The second approach, called quasi-static loading, is to set the total force to the exact value to break the next fiber, and then remove the load before any other fibers break. With this approach it is always one, and only one, fiber breaking for each loading of the system. The same process is repeated until all fibers are broken, making it possible to know the force required to break the fibers after the critical point as well. The critical point is when k_c fibers have broken, and the force required to break that fiber is the highest in the entire breaking process.

Using the quasi-static loading results in the ability to produce strain curves, which describes the total force to break the next fiber when $k-1$ fibers are already broken. When plotting the strain curves the force per fiber σ divided by the spring constant κ will be used

$$\frac{\sigma}{\kappa} = \frac{F}{\kappa N}. \tag{2.4}$$

In (2.4) N is the number of fibers and F is the total force on the system. It is important to note the force per fiber σ is not the force experienced by each intact fiber, but the total force on the system divided by the total number of fibers. The next fiber to break is the fiber requiring the lowest value of σ to break.

2.1.3 Burst Size Distribution

When a fiber breaks, the fraction of the total force previously carried by the broken fiber is distributed among the still intact fibers. How the force is distributed depends on the model and is one of the main differences between different models. Thus, the total force on the bundle required to break the next fiber, F_k, may be less than the total force required to break the previous fiber, F_{k-1}. Multiple fibers breaking without increasing the total force is called a burst, where the number of fibers breaking in a single burst is the burst size Δ. There are several rules defining the size of a burst, and an exclusive burst of size Δ is defined by [9]

$$F_{k+j} < F_k \quad \text{for} \quad j = 1, 2, ..., \Delta - 1, \tag{2.5a}$$
$$F_j < F_k \quad \text{for} \quad j < k, \tag{2.5b}$$
$$F_{k+\Delta} > F_k. \tag{2.5c}$$

In (2.5) F_k is the total force the system is subjected to when failure number k occurs. The condition in (2.5a) is the forward condition, ensuring the total force required to break the $\Delta - 1$ next fibers is lower than the force required to break the first fiber in the burst. The backward condition is given in (2.5b), stating the total force required to break the first fiber in the burst, F_k, is higher than the total force required to break all the previously broken fibers. This ensures that the burst is an exclusive burst, a burst that is not part of a larger burst. (2.5c) is the stopping condition, the total force required to break the next fiber after the burst is finished has to be larger than the total force required to start the burst. The exclusive burst size distribution $D(\Delta)$ is the expected number of exclusive bursts of size Δ for a given system.

2.2 The Equal Load Sharing Model

The equal load sharing model was, as previously mentioned, introduced by Peirce in 1926 [1] and it is the first fiber bundle model. The fraction of the total force previously carried by the failed fibers is distributed equally between the intact fibers, hence the name equal load sharing. It is a mean field theory and it is very easy to simulate on a computer.

2.2.1 Force Redistribution

As the name equal load sharing suggests, the model distributes the total force equally between all the surviving fibers. The force experienced by an intact fiber, $f(\sigma)$, when k fibers are broken is

$$f(\sigma) = \frac{N}{N-k}\sigma. \tag{2.6}$$

The term $N/(N-k)$ in (2.6) increase as the number of broken fibers k increase, causing the intact fibers to experience a higher force for the same force per fiber σ. The effect of the equation for a one dimensional model consisting of $N = 6$ fibers is illustrated in figure 2.1.

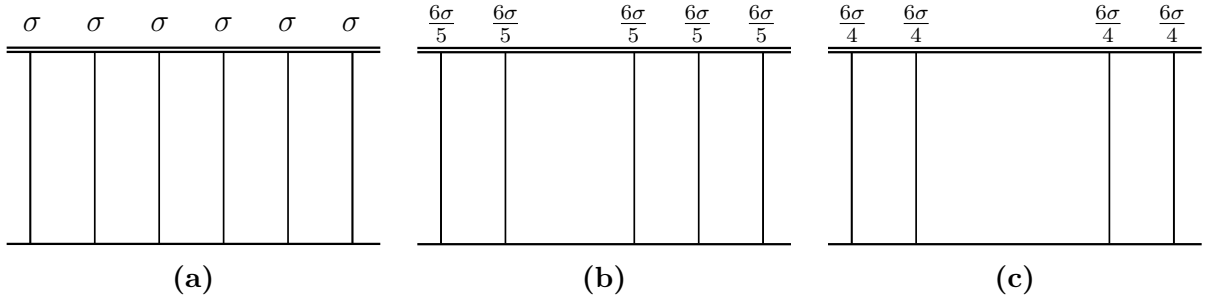

Figure 2.1: The figure shows the redistribution of forces for a one dimensional equal load sharing system consisting of $N = 6$ fibers. The expression above each intact fiber is the force each fiber is subjected to as a function of the force per fiber $\sigma = F/N$, where F is the total force on the system. The figure is reprinted, with permission, from [7].

Distributing the total force like figure 2.1 gives the model a mean field behaviour, where the location of broken and intact fibers does not matter. With no dependency on geometry in (2.6) the breaking order and force required to break the fibers are the same for both one dimensional and two dimensional models. There will however be differences in hole structures and other geometrically dependent quantities. In the model used here the fibers will be arranged in a square pattern, which represents a system of two infinitely stiff plates connected by fibers being pulled apart. Each fiber in the model has four nearest neighbours each, and periodic boundary conditions results in no fibers at a boundary.

2.2.2 Strain Curve

The first fiber to break is the fiber with the lowest threshold extension $\chi_{i,j}$. The next fiber to break is the one with the lowest threshold extension of the remaining fibers, which is the fiber with the second lowest threshold extension in the original bundle. The third fiber to break is the fiber with the third lowest threshold extension, and so on. For the threshold distribution in (2.3) the strain curve can be found analytically by using (2.6) and order statistics. Following the derivation by Hansen et al. in [10] the strain curve in the large system limit is given by

$$\frac{\sigma}{\kappa}\left(\frac{k}{N}\right) = \chi_r \frac{k}{N}\left(1 - \frac{k}{N}\right). \tag{2.7}$$

In the derivation of (2.7) it was assumed the threshold extensions are strictly uniformly distributed. In the large system limit the strictly uniform distribution and the statistical uniform distribution have the same average properties [8], making the expression in (2.7) valid for the average strain curve for large systems. In simulations the strain curve is based on several realisations, and the strain curve should get closer to (2.7) as the number of realisations increase if the system is sufficiently large.

2.2.3 Consecutively Breaking Fibers

For the equal load sharing model the threshold extension for each fiber is drawn from a chosen threshold distribution $P(\chi)$. For an arbitrary realisation of a system, the fiber with the lowest threshold extension has the same probability to be at any of the locations in the system. The same is also true for the fiber with the second lowest threshold extension, and for the one with the third lowest and so on. In the equal load sharing model all fibers experience the same force independent of the configuration, and thus the next fiber to break is always the one with the lowest threshold extension of the still intact fibers. Because of this the average distance between fibers breaking consecutively is just the average distance between two points in a system of the same size. The average distance between two points in a square system of length L in both directions is given by

$$\langle \Delta r^2 \rangle^{1/2} = \left(\frac{\int_{-L/2}^{L/2} \int_{-L/2}^{L/2} (x^2 + y^2) \, \mathrm{d}x\mathrm{d}y}{\int_{-L/2}^{L/2} \int_{-L/2}^{L/2} \mathrm{d}x\mathrm{d}y} \right)^{1/2} = \frac{L}{\sqrt{6}}. \tag{2.8}$$

The average distance between two consecutively breaking fibers is given by (2.8) and is correct during the entire breaking process. For a single realisation of a system, the distance between consecutively breaking fibers are set when the threshold extensions are set. It is thereofre only the average over many samples that will follow (2.8).

2.2.4 Burst Size Distribution

The equal load sharing model with the uniform threshold distribution in (2.3) has a simple parabolic maximum for the average total force $\langle F \rangle$ on the system, which can easily be seen from (2.7). According to the derivation by Hansen et al. in [11] the exclusive burst distribution for such systems follows the power law

$$\frac{D(\Delta)}{N} = C\Delta^{-\xi}, \tag{2.9}$$

where $\xi = 5/2$ and the constant C is system specific. The derivation use the Stirling approximation $\Delta! \approx \Delta^{\Delta} e^{-\Delta} \sqrt{2\pi\Delta}$ [12], which is only valid for large values of Δ, making the result in (2.9) valid only for sufficiently large values of Δ. It was also assumed that the number of fibers in the system N was large in the derivation. The result in (2.9) is valid for a wide range of threshold distributions with a parabolic maximum for the average total force $\langle F \rangle$.

2.3 Other Models

The mean field behaviour of the equal load sharing model is not well suited for a number of physical systems. This section will give a brief introduction to two fiber bundle models without this mean field behaviour, the local load sharing model introduced in 1978 by Harlow and Phoenix [2] and the soft clamp model by Batrouni et al. [6].

2.3.1 The Local Load Sharing Model

The local load sharing model was first introduced more than 50 years after the original equal load sharing model. The models are the extreme opposites of each other, with the local load sharing model distributing the force previously carried by the broken fibers to their nearest intact neighbours. If there is n broken fibers in a single cluster, the fraction of the total force previously carried by these n fibers is distributed equally between the intact fibers which have a member of the hole as nearest neighbour. Using this method of distributing the force, which was used in the original article [2], ensures the model is independent of history. It is possible to end up with an implementation of the model which is dependent of the time if the fraction of force carried by a broken fiber is simply shared equally between the nearest intact fiber at the time of breaking. This is not physical and should be avoided. In two dimensions the fibers are arranged in a square pattern and there are periodiv boundary conditions, just like for the equal load sharing model.

2.3.2 The Soft Clamp Model

The soft clamp model [6] is in between the two extremes of equal and local load sharing. The model consists of two infinite elastic half-planes with linear elastic response connected by elastic fibers, giving two infinitely thick plates with elastic response connected together. With equal properties for both half-planes the the deformation is symmetric about the plane separating the half-planes, making it possible to insert an inifinitely stiff plate at in the middle of the two half-planes without loss of generality. The behaviour of the model is adjusted by adjusting the the stiffness of the half-plane or the spacing of the discretization used. All deformations are linearly elastic, and the fibers are arranged in the same quadratic pattern as the equal and local load sharing model. The size of the simulated systems are finite, and in order to be closer to the infinite system the boundary conditions are periodic.

2.4 The Bridge Model in One Dimension

The fiber bundle bridge model was first introduced by this author in [7] as a specialization project in physics. The two dimensional model, in section 2.5, will use very similar equations and the solution technique will be the same as for the one dimensional model. Since the report from the specialization project is unpublished, the idea behind the model and its derivation are included from [7]. It has been slightly rewritten in addition to changing some of the notation to be consistent with the two dimensional model.

The main idea behind the one dimensional model was to have a model with variable range of interaction, which can be altered by adjusting a parameter. The goal of the model when introduced was to have two different extreme limits. As argued in [7], this was achieved, with the model being a local load sharing model for the softest systems and being equivalent to the equal load sharing model in the limit of stiff systems. The model setup, as seen in figure 2.2, consists of an uniform cable of finite bending rigidity B suspended from an infinitely stiff upper cable by elastic fibers following Hooke's law in (2.1). The upper, infinitely stiff, cable

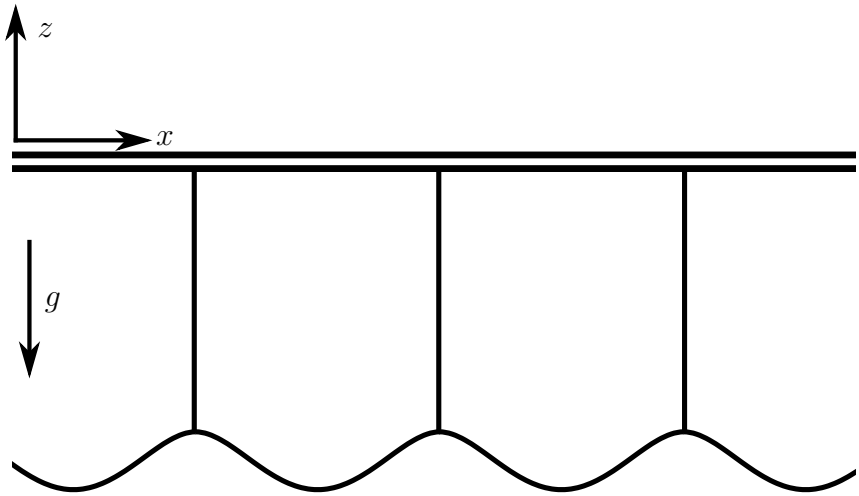

Figure 2.2: The figure shows the setup of the system used for the fiber bundle bridge model in one dimension. A cable of finite bending stiffness B is suspended from an infinitely stiff cable by equidistantly spaced elastic fibers. Gravity acts with a downward force on the bottom cable and the fibers will extend vertically to the point where the system is in equilibrium. The figure is reprinted, with permission, from [7] with some minor modifications.

is held at a constant height and the system is loaded by having the setup in a gravitational field and changing the mass density λ of the cable. The fibers are equidistantly spaced and it is assumed that there are no dynamic effects in the model, much like the equal and local load sharing models.

Every time a fiber breaks all forces are recalculated, the result only depending on which fibers are broken and which are not. This means the model is independent of time, which makes physical sense and is consistent with the equal and local load sharing models and the soft clamp model.

2.4.1 Mathematical Description

The system setup is in the (x, z)-plane, as illustrated in figure 2.2, with the gravitational force working in the negative z-direction. $z(x)$ describes the position, and thus shape, of the bendable cable for a given mass density λ, and with gravity working downwards the extension of fiber k will be

$$\chi = -(z(x_k) - z_0). \tag{2.10}$$

In (2.10) x_k is the horizontal position of fiber number k, and z_0 is the position $z(x)$ of the cable if it was massless, $\lambda = 0$.

All fibers are separated by a distance l in the x-direction, the first fiber is located at $x = 0$, the second at $x = l$ and fiber number k is located at $x = kl$. The model use periodic boundary conditions, and when x reaches a value of Nl in a system of N fibers, the coordinate x starts at zero again.

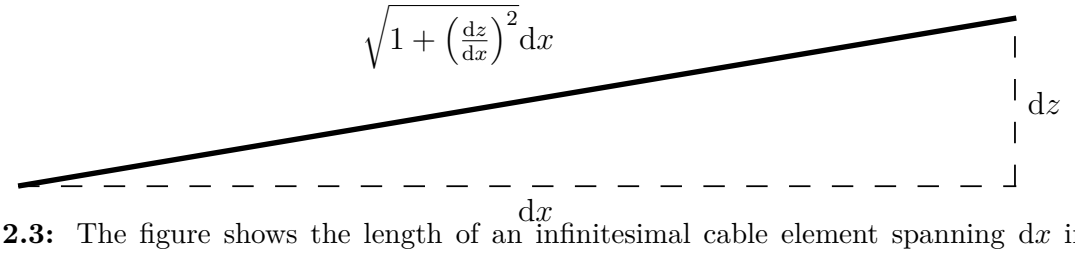

Figure 2.3: The figure shows the length of an infinitesimal cable element spanning $\mathrm{d}x$ in the horizontal x-direction and the change in height over the distance is $\mathrm{d}z$.

An uniform cable with bending stiffness B subjected to a force density $q(x)$ will have a shape given by [13]

$$B\frac{\mathrm{d}^4 z(x)}{\mathrm{d}x^4} = q(x). \tag{2.11}$$

In this model the force density in (2.11) has two different sources. The first source is the force from the gravitational pull on the cable. The cable is assumed to have an uniform mass density λ and the gravitational force density in the z-direction is thus

$$q_g = -g\lambda\sqrt{1+\left(\frac{\mathrm{d}z}{\mathrm{d}x}\right)^2}, \tag{2.12}$$

where the square root is due to the orientation of the cable. The force density $q(x)$ is per length scale in the horizontal direction, and a cable element is in general aligned at an angle with the horizontal axis, as illustrated in figure 2.3. The expression for q_g in (2.12) is found by using trigonometric relations for the cable element in figure 2.3.

The nonlinear form of (2.12) presents a problem when solving the differential equation (2.11). This is taken care of by expanding the square root in (2.12) with respect to $\mathrm{d}z/\mathrm{d}x$ and assuming $\mathrm{d}z/\mathrm{d}x \ll 1$. Then all the terms containing $(\mathrm{d}z/\mathrm{d}x)^{2n}$, where n is an integer larger than zero, can be neglected giving the expression

$$q_g = -g\lambda. \tag{2.13}$$

The parameters in the model can be chosen such that $\mathrm{d}z/\mathrm{d}x \ll 1$ is true when the largest regions of broken fibers in the system is sufficiently small. When this is the case the assumption of neglecting terms containing $(\mathrm{d}z/\mathrm{d}x)^{2n}$ is a good approximation. Later in the simulations, when the holes in the system become sufficiently large, the assumption of small slope may not hold true. In this model (2.13) will still be used in order to be able to solve the system. It is no longer a physically valid assumption, but the model will use it anyway. Care should be taken to choose parameters so that the assumption of $\mathrm{d}z/\mathrm{d}x \ll 1$ is at least valid when all fibers are intact.

The second contribution to the force density $q(x)$ is the force caused by the fibers. Inserting the extension in (2.10) into Hooke's law in (2.1) gives the force from each fiber acting

on the cable. Combining this with the gravitational force density in (2.13) results in the final expression for the shape $z(x)$

$$\frac{\mathrm{d}^4 z(x)}{\mathrm{d}x^4} = -\alpha + \sum_{k=0}^{N-1} f_k \delta\left(x-k\right), \tag{2.14}$$

where the force from fiber number k is $f_k = -\beta(z(k) - z_0)$ if the fiber is intact and zero otherwise. All the variables in (2.14) are dimensionless. The lengths z and x are rescaled with respect to the distance between fiber locations, l, while α and β are defined as

$$\alpha = \frac{g\lambda l^3}{B}, \tag{2.15a}$$

$$\beta = \frac{\kappa l^3}{B}. \tag{2.15b}$$

The value of β will determine the behaviour of the system as it controlls the ratio between spring constant κ of the fibers and the bending rigidity of the cable B. The total force on the system is adjusted by adjusting the value for α, with the mass density, and thus the effective force, increasing for increasing values of β. (2.15) also show halving the length between fibers, $l \to l/2$, is equivalent to increasing the bending rigidity by a factor of eight, $B \to 8B$. This means there are several combinations of l and B which will give rise to the exact same behaviour, and by using (2.15) all the different combinations of l and B giving the same behaviour for a given system size N is covered.

Equation (2.14) is a fourth order ordinary differential equation describing the whole system. Due to the δ-functions in the summation, and the fact that f_k is either proportional to $z(k)$ or zero, depending on wether fiber number k is intact or not, the equation is hard to solve analytically for the whole system. Mathematically the problem is very similar to the Kronig-Penney problem [14] in quantum mechanics. Therefore, the approach used by Hemmer in [14] to solve the Kronig-Penney problem is used to solve (2.14). It solves (2.14) between the fibers, and thus between the δ-functions. Afterwards the solutions between all the fibers are connected using boundary conditions at the fiber locations.

Between two fibers the right hand side of (2.14) is simply $-\alpha$, and the solution between fiber number k and $k+1$, denoted z_k, is given by

$$z_k(x) = -\frac{\alpha}{24}\left(x-k\right)^4 + a_k(x-k)^3 + b_k(x-k)^2 + c_k(x-k) + d_k. \tag{2.16}$$

The constants a_k, b_k, c_k and d_k are unknowns to be determined by the boundary conditions at the fiber locations. The form $(x-k)$ is chosen to make the matrix system nicer than if it had simply been on the form $(x-0)$. The solution in (2.16) is only for the interval from $x = k$ to $x = k+1$, which makes $(x-k)$ zero at the start of each interval and one at the end of each interval. If the form of (2.16) had only been x to the same powers, the constants for each interval would change if the grid was translated a given number of fiber locations. This is impractical and $(x-k)$ is used instead.

There are four unknows per fiber in (2.16), requiring four boundary conditions per fiber. Just like in the Kronig-Penney model, these boundary conditions are found by integrating

the original equation over a small region around the location of the δ-function. Integrating (2.14) over the interval from $x = k - \epsilon$ to $x = k + \epsilon$ and evaluating the answer in the limit $\epsilon \to 0$ yields the first boundary condition

$$\left.\frac{\mathrm{d}^3 z_k}{\mathrm{d}x^3}\right|_{x=k} - \left.\frac{\mathrm{d}^3 z_{k-1}}{\mathrm{d}x^3}\right|_{x=k} = f_k. \tag{2.17}$$

As before $f_k = -\beta(z(k) - z_0)$ for intact fibers and zero for broken fibers. The three remaining boundary conditions can be found by integrating (2.14) over the same interval two, three and four times respectively. Evaluating the results in the limit $\epsilon \to 0$ gives the remaining boundary conditions

$$\left.\frac{\mathrm{d}^2 z_k}{\mathrm{d}x^3}\right|_{x=k} - \left.\frac{\mathrm{d}^2 z_{k-1}}{\mathrm{d}x^2}\right|_{x=k} = 0, \tag{2.18}$$

$$\left.\frac{\mathrm{d}z_k}{\mathrm{d}x}\right|_{x=k} - \left.\frac{\mathrm{d}z_{k-1}}{\mathrm{d}x}\right|_{x=k} = 0, \tag{2.19}$$

$$z_k|_k - z_{k-1}|_k = 0. \tag{2.20}$$

Inserting (2.16) and the expression for f_k into the boundary conditions in (2.17)-(2.20) gives, after some rearranging, the matrix system

$$6a_k - \beta_k d_k - 6a_{k-1} = -\alpha, \tag{2.21a}$$

$$b_k - 3a_{k-1} - b_{k-1} = -\alpha/4, \tag{2.21b}$$

$$c_k - 3a_{k-1} - 2b_{k-1} - c_{k-1} = -\alpha/6, \tag{2.21c}$$

$$d_k - a_{k-1} - b_{k-1} - c_{k-1} - d_{k-1} = -\alpha/24, \tag{2.21d}$$

where β_k is equal to β for intact fibers and zero for broken fibers. The constant z_0 is also set to zero without loss of generality, due to the value of z_0 not changing the equations in (2.21). The only difference for a non-zero value of z_0 is that the whole cable is shifted by a constant amount in the z-direction. All equations in (2.21) are linear, and the matrix for the system will be a $4N \times 4N$ matrix with a corresponding vector of the unknown constants a_k, b_k, c_k and d_k. The value of β_k will only be in the matrix, which means only the matrix will change when a fiber breaks due to the corresponding β_k entry changing from β to zero.

The position of the cable at $x = k$ is always $z_k(k) = d_k$, meaning the extension of fiber number k is $\chi = -d_k$. For a given fiber, d_k may be positive due to the geometry of the problem, which is equivalent to a negative extension χ. This is part of the behaviour of the model, and it is assumed that no fibers will break from negative extension. This assumption stems from the fact that it is always possible to choose a non-zero value for z_0 in order to have $d_k < 0$ for all fibers k without changing the results. In that case there is no negative extension of any fibers, the fibers which would have a negative extension for $z_0 = 0$ is simply compressed. It is assumed the elastic fibers obeys Hooke's law in (2.1) when the fibers are compressed as well as when they are extended, using the same spring constant κ.

2.4.2 Strain Curve

For the equal and local load sharing models the strain curve is the average force per fiber, σ, required to break the next fiber as a function of the fraction of broken fibers k/N. For a given system configuration the force per fiber required to break the next fiber change if the spring constant κ change, however the ratio σ/κ will not. In the bridge model the redistribution of forces is closely linked to the effective spring constant β, and in order to change the behaviour of the system the value of β has to change. For the one dimensional bridge model the ratio α/β will be equivalent to σ/κ in models like the equal and local load sharing models. In the original variables the ratio α/β represents the force per fiber per spring constant, which is the same as σ/κ for the equal and local load sharing models.

The model is linear for a given configuration according to (2.21), making it easy to find the exact value for α required to break the next fiber. Solving the system for $\alpha = 1$ gives the following expression for the value of α required to break the next fiber

$$\frac{1}{\alpha/\beta} = \max_k \left(-\frac{\beta_k d_k}{\chi_k} \right). \tag{2.22}$$

The minus sign in (2.22) ensures only fibers with positive extension $\chi = -d_k$ can be broken, β is still β for intact fibers and zero otherwise and χ_k is the threshold extension of fiber k. Using (2.22) for each fiber breaking gives the strain curve for the given system, as it is the lowest possible force required to break a fiber.

2.4.3 The Equal Load Sharing Limit

From physical intuition the model should become equivalent to the equal load sharing model when the bending rigidity B tends to infinity. To check if this is the case the equations in (2.21) has to be evaluated in the limit of $\beta \to 0$. Since both α and β are directly proportional to B^{-1}, the ratio α/β is held constant as both α and β tends to zero.

First (2.21) is solved analytically for the special case of all fibers intact. The total, dimensionless, force on the system is $N\alpha$ and thus the force per fiber is α. Dividing by the effective spring constant β gives the extension of each fiber, which is

$$\chi = \alpha/\beta. \tag{2.23}$$

All fibers have the same extension given by (2.23), which can be expressed as $z_k(k) = z_{k+n}(k+n)$ where n is an integer. Together with the boundary condition in (2.20) this gives the relation $z_k(k) = z_k(k+1)$. Due to the symmetry the first derivative of z_k has to be zero at both $x = k$ and $x = k+1$. Using these observations together with the expression for z_k in (2.16) yields the solution

$$a_k = \alpha/12, \tag{2.24a}$$
$$b_k = -\alpha/24, \tag{2.24b}$$
$$c_k = 0, \tag{2.24c}$$
$$d_k = -\alpha/\beta. \tag{2.24d}$$
$$\tag{2.24e}$$

Inserting (2.24) into (2.21) for the case of all fibers intact shows that (2.24) is a valid solution of the system of equations. The shape of the cable is determined only by the solution of (2.21) for a given value of α. Of the four equations in (2.21), only (2.21a) contains any information about wether a fiber is broken or not through the value of β_k. For fiber k to break the extension $\chi = -d_k$ has to be finite, as long as the fiber has a finite threshold extension. Assuming the fiber has a finite threshold extension, the expression $\beta_k d_k$ tends to zero in the limit $\beta \to 0$. The new version of (2.21a) is thus

$$a_k - a_{k-1} = 0, \tag{2.25}$$

which does not change dependending on wether fiber number k is broken or not. In this limit the equations in (2.21) does not depend on which fibers are broken and which are intact any more. The value for α tends to zero as well, and the shape of the cable when evaluating (2.24) and (2.16) in this limit, when all fibers are intact, is

$$z_k(x) = -\frac{\alpha}{\beta}. \tag{2.26}$$

The expression in (2.25) also applies for systems with several broken fibers when the bending rigidity B tends to infinity. In the solution in (2.16) the constants α, a_k, b_k and c_k are still zero and the value of d_k is the same constant for all fibers. In this limit the dimensionless force $f_k = -\beta_k d_k$ tends to zero, but that does not mean the actual force tends to zero. The dimensionless extension is a constant $\chi = -d_k = \chi_0$, and the actual force, in its proper units, will be $l\kappa\chi_0$. In order to have a force balance in the system the position of the cable when k fibers are broken will be

$$z_k(x) = -\frac{N}{N-k}\frac{\alpha}{\beta}. \tag{2.27}$$

The expression in (2.27) does not depend on the position x and is constant everywhere. The extension of the fibers is given by $\chi = -z(x)$ from (2.27) and the extension has the exact same form as for the equal load sharing expression, $f(\sigma)/\kappa$, in (2.6). This further supports the notion the equivalent to σ/κ is α/β in the one dimensional bridge model.

2.5 The Bridge Model in Two Dimensions

The one dimensional bridge model was discovered to have an adjustable effective range of interaction and it becomes equivalent to the equal load sharing model when the bending rigidity of the cables tends to infinity. The two dimensional model will based on the one dimensional model, as the variable range of interaction in the one dimensional model is desired to have for the two dimensional model as well. The model will consist of cables from the one dimensional model constructing a square mesh pattern with a fiber located at each intersection of the cable. It will be a very thin, bendable plate with many square holes in it.

2.5.1 Mathematical Description

In two dimensions the model is a system of one dimensional cables arranged in a square mesh pattern. At the intersection of two crossing cables there is a joint keeping them at the same vertical position, but the joint is designed in such a way that there is no torsional force on the cables due to the joint. That ensures even if the cable in one direction has a relatively steep slope, the cable crossing in the perpendicular direction is not affected by this. It is only affected by the vertical position of the joint.

The cables are arranged in a square pattern with indexing following the notation used in figure 2.4b. From the figure it is also easy to see that there are two cable elements of unit, dimensionless length for each fiber, which is twice as many as in the one dimensional model. The cables will behave like connected one dimensional models, and an example of a $N = 3^2$ system with all its fibers intact can be seen in figure 2.4a. In the figure the positive z-direction is up and gravity is working in the opposite direction, just like in the one dimensional model.

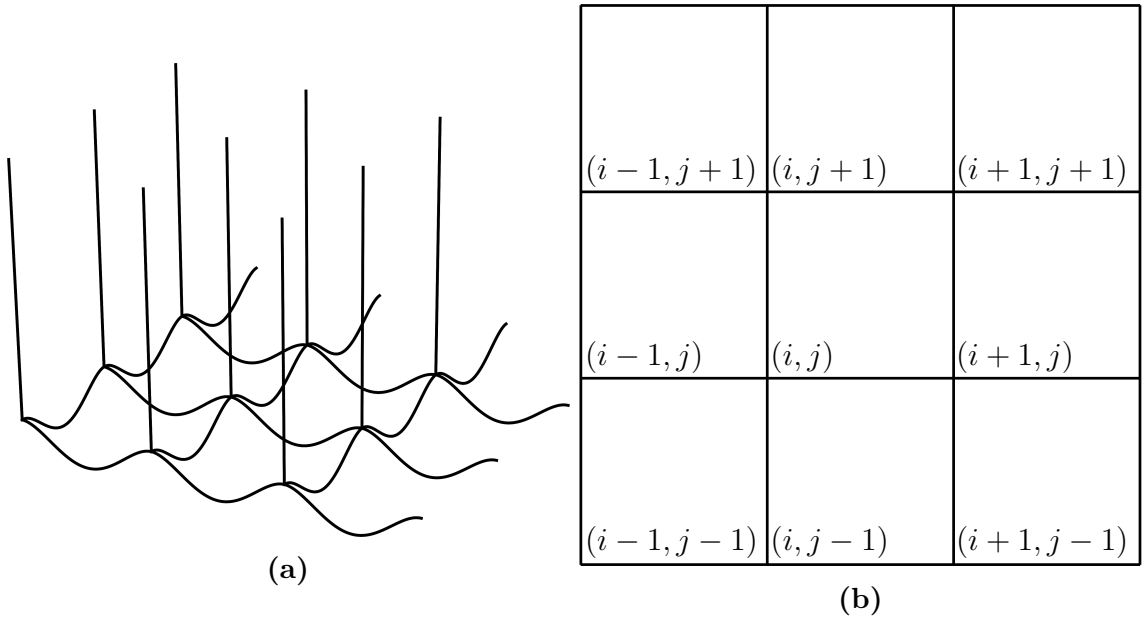

Figure 2.4: Figure (a) shows a three dimensional illustration of a given system consisting of $N = 3^2$ fibers, where all fibers are intact and periodic boundary conditions are used. The fibers are aligned along the z-axis and the cables are aligned along the x- and y-directions. Figure (b) illustrates the convention used in this text when indexing the fiber locations. The notation is (i, j) where i is the dimensionless position in the x-direction and j is the dimensionelss position in the y-direction.

As already mentioned, the two dimensional model consists of several interconnected instances of one dimensional models. The different instances of the one dimensional models are connected in the way figure 2.5 shows. The distance between the cables is just for illustration purposes, and in the equations the distance is set to zero. The cables are subject to the gravitational force density q_g given by (2.13), which is valid when the slopes of the

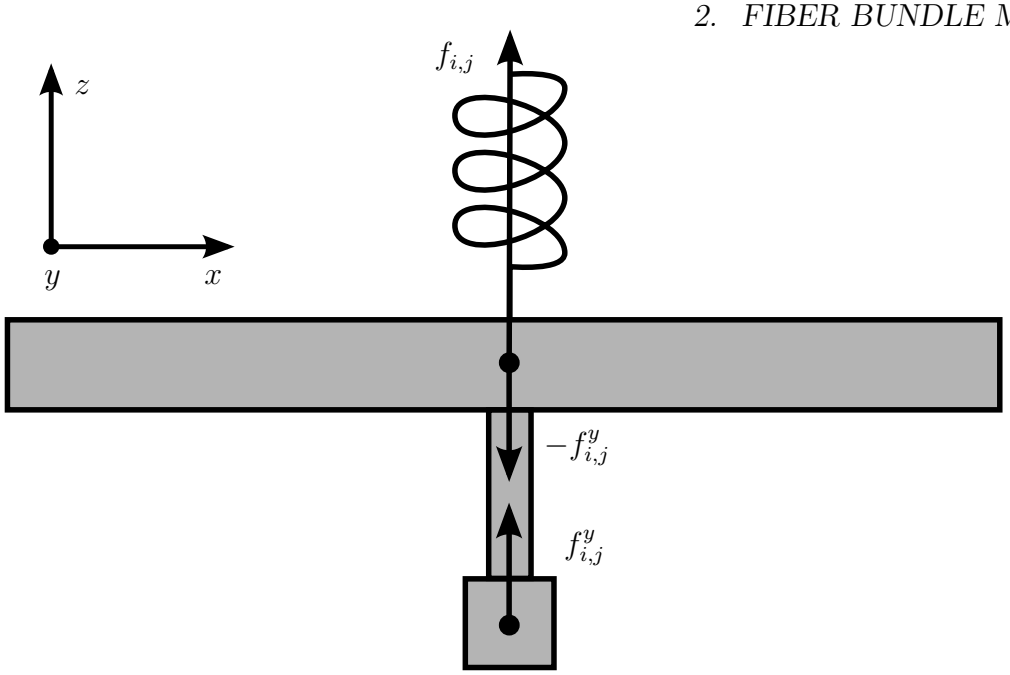

Figure 2.5: The figure shows a schematic drawing of the forces acting at the location of fiber (i, j). The distance between the cables is only for illustration purposes, making it easier to see which force acts on which object. The distance between the two force centers is set to zero in the model. The upwards force is the force from the elastic fiber, $f_{i,j}$, and the force on the cable aligned along the y-direction is $f^y_{i,j}$ and the force experienced by the cable aligned along the x-direction will be denoted $f^x_{i,j}$. In this illustration the gravitational force is not included.

cables are much smaller than one. As in the one dimensional model the assumption may fail when a large fraction of the fibers in the system are broken, but the same expression for the gravitational force will be used anyway.

The form of the force term due to the fibers has changed compared to the one dimensional model. There is two elements per cable now, and the force on each of the two intersecting cables at the location of a failed fiber is different from zero in general. Looking at figure 2.5 the force balance can be set up, giving

$$f^x_{i,j} + f^y_{i,j} = f_{i,j} = \beta_{i,j}\chi, \tag{2.28}$$

where $f^x_{i,j}$ is the force experienced by the cable in the x-direction. $\beta_{i,j}$ is equal to β for intact fibers and zero otherwise and χ is the extension of the fiber in question.

Inserting the new forces from (2.28) in to the equation for the one dimensional system, (2.14), yields the following system of equations describing the two dimensional model

$$\frac{\mathrm{d}^4 z^x_j(x_j)}{\mathrm{d}x^4_j} = -\alpha + \sum_{i=0}^{L-1} f^x_{i,j}\delta(x_j - i), \tag{2.29a}$$

$$\frac{\mathrm{d}^4 z^y_i(y_i)}{\mathrm{d}y^4_i} = -\alpha + \sum_{j=0}^{L-1} f^y_{i,j}\delta(y_i - j). \tag{2.29b}$$

The notation used in (2.29) needs some explaining. z_j^x is the shape of the cable aligned along the x-direction located at $y = j$ in the coordinate system. Likewise, z_i^y is the shape of the cable aligned along the y-direction located at $x = i$ in the coordinate system. $f_{i,j}^x$ and $f_{i,j}^y$ is the force experienced by the cable in the x- and the y-direction respectively, and they obey (2.28). The number of fibers in each direction is L, with $N = L^2$ being the total number of fibers in the system. There is one equation for each cable in the system, giving a total of $2L$ equations, one for each value of i and one for each value of j. The dimensionless variables α and β are defined the same way as in the one dimensional model, and the definition can be found in (2.15). The distance between fibers l, the beding rigidty B and the mass density λ are chosen to be equal for all the cables in all directions for simplicity. It is possible to have cables with different properties for the different directions and for each cable, but new dimensionless equations would have to be found from the original equations with dimension.

Due to the cables being connected by a joint at each fiber location (i, j), where the fibers intersect one another, the cables are required to be at the same height at this point which results in the condition

$$z_j^x(i) = z_i^y(j). \tag{2.30}$$

The distance between the center of each cable in figure 2.5 is thus set to zero. The equations in (2.29) are solved between fibers using the same approach as in section 2.4.1. After solving the equations the condition in (2.30) is inserted directly into the solution, giving the final expressions for the vertical position of the cables

$$z_{i,j}^x(x_j) = -\frac{\alpha}{24}(x_j - i)^4 + a_{i,j}^x(x_j - i)^3 + b_{i,j}^x(x_j - i)^2 + c_{i,j}^x(x_j - i) + d_{i,j}, \tag{2.31a}$$

$$z_{i,j}^y(y_i) = -\frac{\alpha}{24}(y_i - j)^4 + a_{i,j}^y(y_i - j)^3 + b_{i,j}^y(y_i - j)^2 + c_{i,j}^y(y_i - j) + d_{i,j}. \tag{2.31b}$$

In (2.31) $z_{i,j}^x$ denotes the vertical position of the cable element between fiber (i, j) and fiber $(i + 1, j)$ and $z_{i,j}^y$ denotes the vertical position of the cable element between fiber (i, j) and $(i, j + 1)$. Note that the condition in (2.30) is satisfied by having the same constant $d_{i,j}$ in both (2.31a) and (2.31b). The cables are continuous in each direction, making the $d_{i,j}$ in both equations adequate to satisfy (2.30) for all possible realisations of the system.

There are nine different unknowns in the system for each fiber at this point, which requires nine equations per fiber to find the solution. Two of the unknowns per fiber are $f_{i,j}^x$ and $f_{i,j}^y$ in (2.28), and the rest are the coefficients in (2.31). The first equation comes from inserting the expression for χ for each fiber into (2.28), giving

$$f_{i,j}^x + f_{i,j}^y = f_{i,j} = -\beta_{i,j} d_{i,j}. \tag{2.32}$$

The eight other equations comes from integrating each of the equations in (2.31) in a small area around the fiber four times each, giving eight boundary conditions. This is the same approach that was used to find the boundary conditions in (2.17)-(2.20), and the eight

resulting boundary conditions are

$$\left.\frac{\mathrm{d}^3 z^x_{i,j}}{\mathrm{d}x_j^3}\right|_{x_j=i} - \left.\frac{\mathrm{d}^3 z^x_{i-1,j}}{\mathrm{d}x_j^3}\right|_{x_j=i} = f^x_{i,j}, \tag{2.33a}$$

$$\left.\frac{\mathrm{d}^3 z^y_{i,j}}{\mathrm{d}y_i^3}\right|_{y_i=j} - \left.\frac{\mathrm{d}^3 z^y_{i,j-1}}{\mathrm{d}y_i^3}\right|_{y_i=j} = f^y_{i,j}, \tag{2.33b}$$

$$\left.\frac{\mathrm{d}^2 z^x_{i,j}}{\mathrm{d}x_j^2}\right|_{x_j=i} - \left.\frac{\mathrm{d}^2 z^x_{i-1,j}}{\mathrm{d}x_j^2}\right|_{x_j=i} = 0, \tag{2.33c}$$

$$\left.\frac{\mathrm{d}^2 z^y_{i,j}}{\mathrm{d}y_i^2}\right|_{y_i=j} - \left.\frac{\mathrm{d}^2 z^y_{i,j-1}}{\mathrm{d}y_i^2}\right|_{y_i=j} = 0, \tag{2.33d}$$

$$\left.\frac{\mathrm{d}z^x_{i,j}}{\mathrm{d}x_j}\right|_{x_j=i} - \left.\frac{\mathrm{d}z^x_{i-1,j}}{\mathrm{d}x_j}\right|_{x_j=i} = 0, \tag{2.33e}$$

$$\left.\frac{\mathrm{d}z^y_{i,j}}{\mathrm{d}y_i}\right|_{y_i=j} - \left.\frac{\mathrm{d}z^y_{i,j-1}}{\mathrm{d}y_i}\right|_{y_i=j} = 0, \tag{2.33f}$$

$$\left.z^x_{i,j}\right|_{x_j=i} - \left.z^x_{i-1,j}\right|_{x_j=i} = 0, \tag{2.33g}$$

$$\left.z^y_{i,j}\right|_{y_i=j} - \left.z^y_{i,j-1}\right|_{y_i=j} = 0. \tag{2.33h}$$

Inserting the solution for $f^x_{i,j}$ from (2.32) and the expressions for the positions of the cables from (2.31) give

$$6a^x_{i,j} + \beta_{i,j} d_{i,j} + f^y_{i,j} - 6a_{i-1,j} = -\alpha, \tag{2.34a}$$

$$6a^y_{i,j} - f^y_{i,j} - 6a^y_{i,j-1} = -\alpha, \tag{2.34b}$$

$$b^x_{i,j} - 3a^x_{i-1,j} - b^x_{i-1,j} = -\alpha/4, \tag{2.34c}$$

$$b^y_{i,j} - 3a^y_{i,j-1} - b^y_{i,j-1} = -\alpha/4, \tag{2.34d}$$

$$c^x_{i,j} - 3a^x_{i-1,j} - 2b^x_{i-1,j} - c^x_{i-1,j} = -\alpha/6, \tag{2.34e}$$

$$c^y_{i,j} - 3a^y_{i,j-1} - 2b^y_{i,j-1} - c^y_{i,j-1} = -\alpha/6, \tag{2.34f}$$

$$d_{i,j} - a^x_{i-1,j} - b^x_{i-1,j} - c^x_{i-1,j} - d_{i-1,j} = -\alpha/24, \tag{2.34g}$$

$$d_{i,j} - a^y_{i,j-1} - b^y_{i,j-1} - c^y_{i,j-1} - d_{i,j-1} = -\alpha/24. \tag{2.34h}$$

Like in the one dimensional model, described by the matrix system in (2.21), the information about wether a fiber is broken or not is only present in the matrix. Compared to the one dimensional model, the new model has twice the number of unknowns per fiber and thus twice the number of equations, and the matrix have the size $8N \times 8N$.

2.5.2 Strain Curve

In section 2.4.2 it was established that the strain curve for the bridge model should be relatable to the strain curves of the equal and local load sharing models. In the one dimensional problem there were N cable elements of unit, dimensionless length, resulting in the force per

fiber being α. For two dimensions there are two such cable elements per fiber, and the force per fiber is thus 2α. Therefore, the strain curve is given by $2\alpha/\beta$, which is equivalent to σ/κ in the equal and local load sharing model. If the system is solved for $\alpha = 1$ the value of $2\alpha/\beta$ required to break the next fiber, and thus the strain curve, is given by

$$\frac{1}{2\alpha/\beta} = \max_{i,j}\left(-\frac{\beta_{i,j}d_{i,j}}{2\chi_{i,j}}\right), \tag{2.35}$$

which is a slightly modified edition of (2.22). The search for the maximum value in (2.35) includes all combinations of i and j. $\chi_{i,j}$ is the threshold extension for fiber (i,j) and $\beta_{i,j}$ is equal to β for intact fibers and zero for broken fibers. The two different possible values for $\beta_{i,j}$ ensures only intact fibers can be chosen as the maximum, and the minus sign ensures only fibers with positive extension $\chi = -d_{i,j}$ can break.

2.5.3 The Equal Load Sharing Limit

In section 2.4.3 it was shown that the one dimensional bridge model is equivalent to the equal load sharing model in the limit $B \to \infty$. Since the two dimensional model consists of several interconnected instances of the one dimensional model, it is expected to be equivalent to the equal load sharing model in the same limit as well. Using the same approach as in section 2.4.3, the limit $B \to \infty$ will be checked for the two dimensional model in this section.

First, the solution to (2.34) in the case of all fibers intact is found by use of symmetry. Due to the symmetry in the problem the extension of all fibers is the same. With $2N$ cable elements of unit dimensionless length, the extension of all fibers will be

$$\chi = -2\frac{\alpha}{\beta}. \tag{2.36}$$

When all fibers are intact, the highest point of each cable are at the fiber locations. Thus, the first derivative of the vertical positions of all the cables have to be zero. Using this together with the boundary conditions in (2.33e)-(2.33h) gives the solution

$$a^x_{i,j} = a^y_{i,j} = \alpha/12, \tag{2.37a}$$
$$b^x_{i,j} = b^y_{i,j} = -\alpha/24, \tag{2.37b}$$
$$c^x_{i,j} = c^y_{i,j} = 0, \tag{2.37c}$$
$$d_{i,j} = -2\alpha/\beta, \tag{2.37d}$$
$$f^x_{i,j} = f^y_{i,j} = \alpha, \tag{2.37e}$$

The constants in (2.37) satisfies the matrix equation in (2.34), and is thus a valid solution of the system. The expression for the forces, $f^x_{i,j}$ and $f^y_{i,j}$, is found after the other coefficients in (2.37) by inserting the already found coefficients into (2.32) and (2.34b). The result in (2.37e) can also be found by symmetry arguments. An example of this is that the system when all fibers are intact can be thought of as a system of independent one dimensional models with all fibers intact and effective spring constant $\beta/2$, due to the two cables per fiber.

As in section 2.4.3, the limit of infinite bending rigidity B is evaluated by letting both α and β tend to zero while keeping α/β constant. Doing so gives the following expressions for the position of the cables when all fibers are intact

$$z^x_{i,j}(x_j) = -2\frac{\alpha}{\beta}, \tag{2.38a}$$

$$z^y_{i,j}(y_i) = -2\frac{\alpha}{\beta}. \tag{2.38b}$$

According to (2.38) all cables are at the same height everywhere in the system, creating a square mesh pattern at a constant height. This is effectively an infinitely stiff plates full of square holes. The expressions in (2.38) comes from inserting the values for the constants in (2.37) evaluated in the limit $B \to \infty$ into (2.31). All the constants in (2.37) is zero except for $d_{i,j}$, which is constant for a given value of α/β.

In the matrix equation in (2.34) only the first equation, (2.34a), change depending on wether a fiber is broken or not. If the fiber is broken then $\beta_{i,j} = 0$ and if not the value is $\beta_{i,j} = \beta$. For the fiber at location (i, j) to break the extension $\chi = -d_{i,j}$ has to be finite as long as the threshold extension $\chi_{i,j}$ is finite. Assuming all fibers have a finite threshold extension, the expression $\beta d_{i,j}$ tends to zero in the limit $\beta \to 0$. The new version of (2.34a) is thus

$$6a^x_{i,j} + f^y_{i,j} - 6a_{i-1,j} = 0, \tag{2.39}$$

while all other equations in (2.34) does not change other than the right hand side tending to zero since α tends to zero in this limit. The condition on the force in (2.32) also change and become

$$f^x_{i,j} + f^y_{i,j} = 0. \tag{2.40}$$

Using the solution for (2.34) when all fibers are intact in the limit of infinite bending rigidty B gives the following result when k fibers are broken

$$a^x_{i,j} = a^y_{i,j} = 0, \tag{2.41a}$$

$$b^x_{i,j} = b^y_{i,j} = 0, \tag{2.41b}$$

$$c^x_{i,j} = c^y_{i,j} = 0, \tag{2.41c}$$

$$d_{i,j} = -\chi_0, \tag{2.41d}$$

$$f^x_{i,j} = f^y_{i,j} = 0. \tag{2.41e}$$

Inserting (2.41) into the expression for the position of the cables in (2.31) will give a constant expression just like in (2.38), the only difference is the extension $\chi = -d_{i,j}$, which can have any value and still satisfy the matrix equation in (2.34) in the limit of infinite bending rigidity. The dimensionless force tends to zero, but the actual force, in its proper units, is not zero. The extension when k fibers are broken is given by the constant $\chi = \chi_0$, and the value can be found by setting up the force balance for the whole system. The total dimensionless force on the system will always be $2N\alpha$ and each intact fiber is subjected to a force $\beta\chi_0$. Setting up the force balance when k fibers are broken and rearranging gives

$$\chi_0 = 2\frac{N}{N-k}\frac{\alpha}{\beta}. \tag{2.42}$$

As argued in section 2.5.2 $2\alpha/\beta$ is equivalent to σ/κ in the equal and local load sharing model. The extension for each fiber is thus equal to the extension $f(\sigma)/\kappa$ in the equal load sharing model, given in (2.6). This means the two dimensional bridge model is equivalent to the equal load sharing model in the limit of infinite bending rigidity B.

3 Simulations and Algorithms

Most of the programs used were written in C/C++ for superior speed compared to non-compiling languages. In order to be sure to get the precision required all floating point numbers where represented by 64 bits. The machine epsilon for 64 bit numbers is in the order of 10^{-16}, and this is considered when the parameters are chosen for the bridge models.

Section 3.1 briefly explains the implementation of the equal load sharing model, while section 3.2 gives an overview of how the bridge model was implemented. Lastly, the cluster finding algorithm is outlined in section 3.3.

3.1 The Equal Load Sharing Model

In the equal load sharing model the weakest fiber breaks first, then the next weakest and so on. All fibers are given a random threshold extension at the start and by sorting the fibers according to threshold value the fibers are automatically in the order in which they will be broken. The implementation used here stores the location and threshold extension of a fiber in a struct, and the `std::sort` function in C++ is used with a custom criterion to sort by. The custom criterion is a function making `std::sort` sort the structs by the threshold extensions and not by location.

3.2 The Bridge Model

When simulating the breaking process for the bridge model in two dimensions the most time consuming part is to solve the matrix equation given by (2.34). Each time a fiber breaks the matrix equation has to be solved again in order to determine which fiber breaks next and at which value of α it happens. The matrix from (2.34) is a very sparse matrix with only $31N$ out of $64N^2$ elements possibly different from zero in a system of $N = L^2$ fibers. When all fibers are intact the number of non-zero values is exactly $31N$, but for each fiber breaking the number of non-zero elements deacrease by 1 because of $\beta_{i,j}$ going from β to zero for the broken fiber.

The final implementation used for all the results in chapter 4 is outlined in section 3.2.1. Section 3.2.2 contains a short description of the methods that did not work out and the reason they were not chosen for the final implementation.

3.2.1 Implementation

The program has two main parts, first the matrix equation in (2.34) has to be solved each time a fiber break and afterwards the next fiber to break has to be found. There are N fibers in a system and (2.34) has to be solved N times in order to break the system, which is the most time consuming part of the simulations. To save a little time the analytical solution when all fibers are intact, given in (2.37), is used when breaking the first fiber, saving one solving of the matrix equation.

To solve the matrix the remaining $N-1$ times the function `spsolve` in the Armadillo library [15] is used. This is a sparse, direct matrix solver, which makes it faster than a general direct solver. Only the non-zero elements are stored and the solver knows which elements are always zero and which are not. Using a sparse solver helps with memory usage as well, which will quickly outgrow the size of readily available computer memory at the time of writing. For a system consisting of $N = 100^2$ fibers the needed storage to store the whole matrix with all zero elements as 64 bit numbers would be 51.2 gigabytes for only the numbers. With the sparse solver only 2.48 megabytes are required to store the numbers in the matrix, which is a lot less than 51.2 gigabytes. The biggest problem with `spsolve` is that it is still a direct solver, which becomes very slow when the matrix size is sufficiently large. It is still faster than the other methods that have been tried up to this point.

The second part of the program is to find the next fiber to break and the corresponding value for α. To find this fiber (2.35) is used, which means all intact fibers has to be checked against each other. Then the next fiber is broken and the matrix has to be updated to reflect this, and the process starts over with solving the matrix problem for the updated matrix.

The `spsolve` function can be run in parallel on the processor, but since the search for the weakest fiber is not parallelized, this was not done. Instead, several different instances of the program was run simultaneously at different cores of the processor. When the program is not highly parallelizable, this is an easy way of utilizing more of the processor and getting more results quicker.

3.2.2 Numerical Methods That Did Not Work

For large sparse matrix systems iterative solvers are often faster than the direct solvers. A lot of time was spent implementing and trying different iterative solvers, but none of them resulted in a faster program than the one outlined in section 3.2.1. Two methods were tried in particular, the conjugate gradient method [16] and the successive over relaxation method (SOR) [17]. The SOR method is not a very fast and clever method compared to the conjugate gradient method, but if it works well enough it is potentially possible to use the multi grid framework [18]. Multi grid methods use several grids of different sizes and restricts and interpolates between them, giving a large speed up for well suited problems.

The first method to be implemented was the Hestenes-Stiefel version of the conjugate gradient method [19]. The method requires the matrix in the problem to be symmetric and positive definite, none of which is true for the matrix in (2.34). The conjugate gradient normal equation error method (CGNE) [20] is used to overcome this problem, where the matrix is multiplied by its own transpose. The resulting matrix is a little less sparse than

the original matrix, but it is still very sparse and it is possible to find all the coefficients by hand. This was done and implemented following [19] with the matrix stored implicitly. When all fibers are intact in the system the algorithm is fast, but as soon as fibers start to break the convergence is very slow. As more and more fibers break the convergence get worse and worse, and it gets even worse as the value of β decrease.

The second method implemented was the SOR method. In order to have convergence to the solution the same normal equation that was used in the conjugate gradient method was used here as well. The method was implemented directly from [17] and for larger values of β, like $\beta = 1$, the rate of convergence is decent. However, as the value for β decrease, making the system stiffer, the convergence become even more horrible than for the conjugate gradient method. Therefore, a proper attempt at the multi grid framework was never prioritised.

With a good preconditioner the conjugate gradient method should be able to perform well, but this author has not found one yet. Even though the implementation gives the right answer eventually, it is very easy to get a bug in the program slowing down the rate of convergence. It is possible the implementations that were tried had this bug, and was slower because of this. The SOR method performed much worse than the conjugate gradient method. Ideally a good preconditioned conjugate gradient method free of bugs should be implemented, hopefully outperforming `spsolve` by a good margin.

3.3 Cluster Finding Algorithm

For two dimensional models it is possible to have two dimensional regions of broken fibers where all fibers have at least one broken fiber as one of its nearest neighbours. These clusters of broken fibers are called holes, and it is of interest to know the hole structures and number of holes there are in total. A well known algorithm to do this is the one presented by Hoshen and Kopelman in [21]. The algorithm use a clever labelling of the locations of the broken fibers, which are members of a hole, and it makes it possible to determine the hole structure by looking at each fiber only once.

The algorithm presented by Hoshen and Kopelman in [21] iterates through all the fibers each time the algorithm is run. In the fiber bundle models it is desireable to know the hole strucure at all time steps, meaning each time a fiber breaks the holes has to be found. If all broken fibers have a label, the hole structure is known for the given system. When the next fiber breaks there is only only a few different possibilities for how the hole structure can change. Either the new fiber breaking is surrounded by intact fibers, which means it is a completely new hole, or it has one or more neighbours part of a hole. If the neighbouring fibers are part of different holes, the two holes has to be merged first. The fiber that broke is part of the existing hole and gets a corresponding label. This approach was used by Dahle in [22, 23], and it has a straight forward implementation of low complexity.

3.3.1 Implementation

The labels are kept in an array where each index corresponds to a specific fiber, and initally all labels are set to the chosen default value for intact fibers, which is -1 in this case. The

labels keep track of which fiber is part of which hole, and all holes has a single root fiber. The root fibers are special due to the labels being the same as the index originally given to the fibers. This makes them easy to identify, since all other fibers have a label different from the index.

The first fiber to fail is a special case due to it being the only broken fiber in the system. It is therefore the only member of the only hole in the system, giving it a label equal to the index of the fiber. After the first fiber has failed, all the neighbours of the fibers failing aferwards will have to be checked. If the newly failed fiber has no neighbours which are broken, the label is set to the index making the fiber a new root. If a fiber is nearest neighbour to one, and only one, hole the label of the newly broken fiber is set to the label of the existing hole. If there are two or more nearest neighbours part of different holes, the holes have to be merged to a new, larger hole. This is done by finding the root of all the holes and then choosing which root should be the root of the new hole. The label of the other roots are set to the label of the chosen root, resulting in the larger hole only having one root as it should be. The label of newly broken fiber is set to the root of the large hole.

A demonstration of the labelling process is presented in figure 3.1. The illustration does not represent the exact steps of the simulation, but it illustrates how the labels are determined and how holes are merged together. It is a given example configuration of a system where three fibers are broken and assigns a label for each broken fiber separately, starting from the bottom left. The red square is the broken fiber which will be given a label next, grey fibers are intact and each assigned label is represented by a color different from the previously mentioned colors. In figure 3.1a there are no fibers with already assigned labels, and the fiber is a new root. The indexing starts in the lower left corner and goes to the right, making the index of the broken fiber in question 8. The next fiber in question in figure 3.1b does not have a neighbour with already assigned label either, and it is a root with label 12. The last broken fiber, in figure 3.1c has two neighbours, each with a different root. The roots of the neighbouring fibers are 8 and 12, and 8 is chosen as the new root. This results in the new fiber getting the label 8, and the fiber with index 12 is changed from a root to a member of the hole with root label 8. The final labels for the example system are found in figure 3.1d.

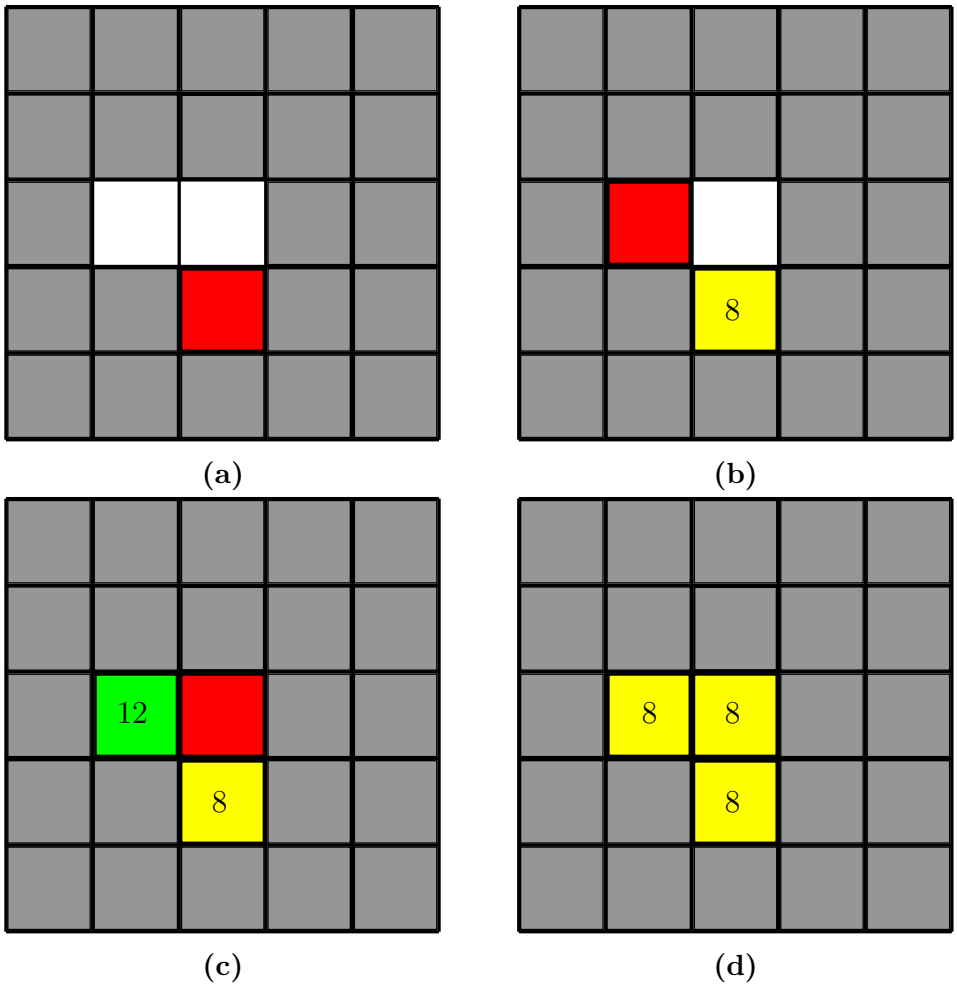

Figure 3.1: The figures shows the labeling process in the slightly modified Hoshen-Kopelman algorigthm. The scan, and indexing, of the fibers start in the lower left corner, with increasing indicies to the right. The red square is the broken fiber that will be assigned a label to next, and each label has its own color for illustration purposes. In figure (a) and (b) the broken fiber under consideration does not have a neighbour which has been assigned a label yet. Therefore, they get a label equal the index of the fiber. In (c) the broken fiber in question has two neighbours which are part of different holes, and the holes has to be merged together. (d) shows the end result after the scan of the system.

4 Restults

In this section the results from both the equal load sharing model and the two dimensional bridge model are presented. The two models use the same number of samples for the same system size in order to base the average values on the same number of broken fibers. Due to the substantially longer time required to simulate the bridge model compared to the equal load sharing model, the number of samples and the system sizes are determined by what is realistically possible for the bridge model. The main results will be based on systems of $N = 50^2$ fibers with 500 realisations for each choice of parameters. Some minor results are also given for 3125 sampels of a system with $N = 20^2$ fibers in order to compare the behaviour of the bridge model for different values of β and system sizes N. With 3125 samples for the system consisting of $N = 20^2$ fibers, the total number of broken fibers is the same as for 500 samples for a system with $N = 50^2$ fibers. This was done in order to base all results on the same number of broken fibers.

In section 4.1 the results for the equal load sharing model are presented. The results for the two dimensional bridge model are presented in section 4.2. All results, indpendent of system size N and wether it is equal load sharing or bridge model, use the flat threshold distribution $P(\chi) = \chi/0.001$.

4.1 The Equal Load Sharing Model

The results in this section are based on 500 samples for a system consisting of $N = 50^2$ fibers. As previously mentioned, the time used to break one realisation of the system is small, but the number of realisations and system size are chosen to be the same as for the bridge model.

The strain curve for the equal load sharing model with the threshold distribution $P(\chi) = \chi/0.001$ is well known for large systems, and is given in (2.7). This curve can be seen in red in figure 4.1 together with the strain curve from the simulations. The strain curve from the simulations is the average of σ/κ required for failure number k to happen in each realisation of the system.

The average distance between consecutively breaking fibers, $\langle \Delta r^2 \rangle^{1/2}$, in the equal load sharing model should be the average distance between two fibers in the system if the implementation is correct. Figure 4.2 shows the average distance between consecutively fibers based on the 500 realisations of the system with $N = 50^2$ fibers together with the theoretical result given by (2.8).

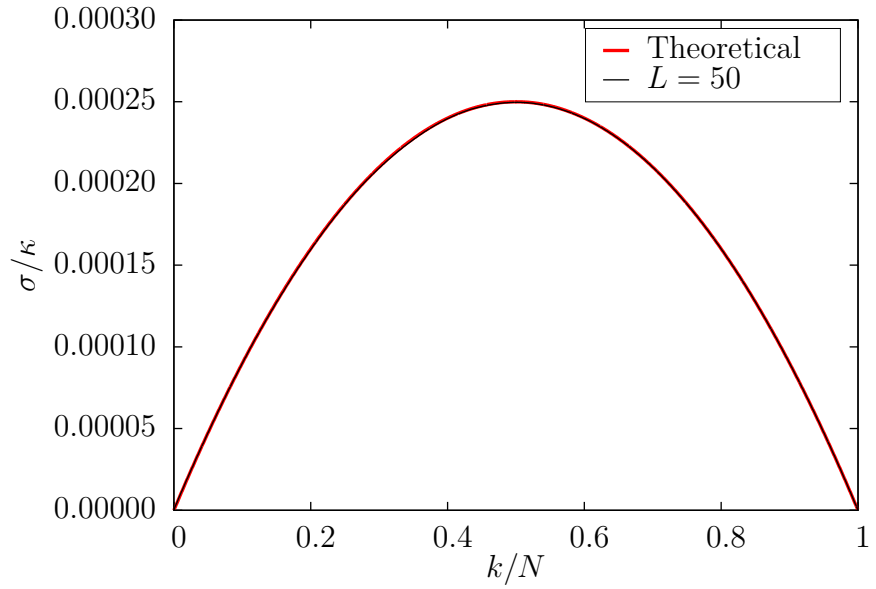

Figure 4.1: The figure shows the theoretical strain curve, in red, for the equal load sharing model given in (2.7) and the strain curve from the simulations. The system in question has $N = 50^2$ fibers and 500 realisations were used to find the average value for each point in the strain curve.

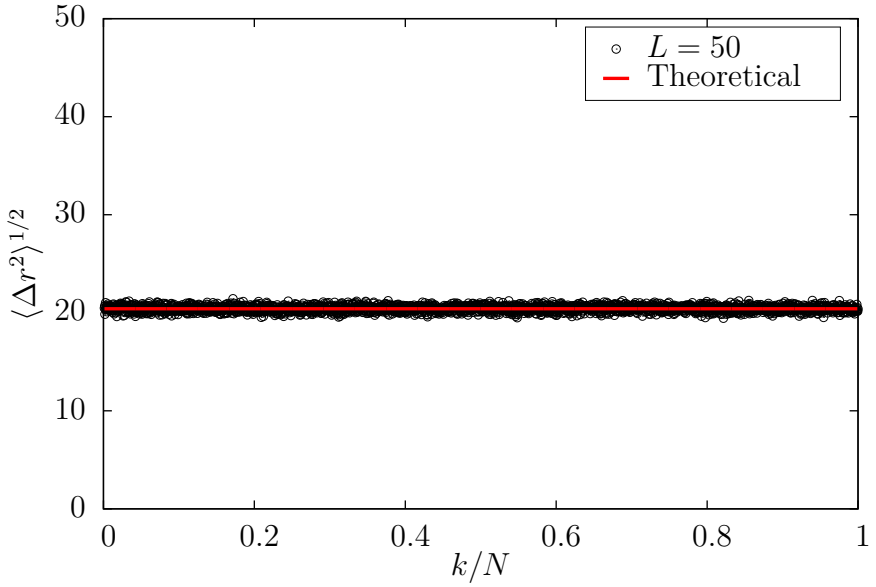

Figure 4.2: The figure shows the average distance between consecutively breaking fibers, $\langle \Delta r^2 \rangle^{1/2}$, for the equal load sharing model. The system in question has $N = 50^2$ fibers and the plot is the average of 500 samples. The red line in the figure is the theoretical result given by (2.8).

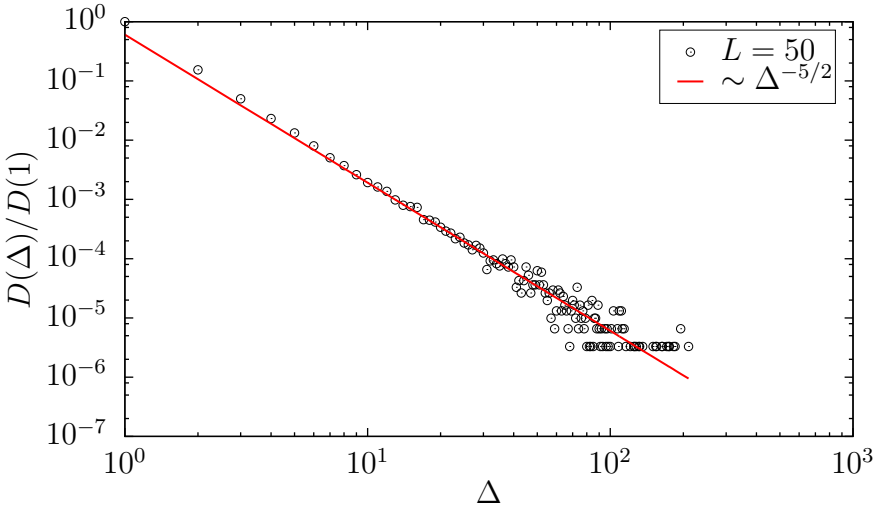

Figure 4.3: The figure shows the burst size distribution based on 500 samples for an equal load sharing system consisting of system of $N = 50^2$ fibers. The burst size distribution is represented by the black circles, and the theoretical burst size distribution in (2.9) with exponent 5/2 is represented by the straight red line in the plot. The constant C in (2.9) is manually chosen to fit the data reasonably well, and the power law is for reference only.

The burst distribution $D(\Delta)$ for the equal load sharing model should follow the power law in (2.9) for sufficiently large bursts. As was mentioned in section 2.2.4 the exponent of the burst size distribution is $\xi = 5/2$ for the equal load sharing model for the flat threshold distribution $P(\chi) = \chi/0.001$. Figure 4.3 shows the burst size distribution averaged over the 500 samples for the system, and the power law in (2.9) with exponent $\xi = 5/2$ is manually fitted as a line of reference.

4.2 Bridge Model

For the fiber bundle bridge model introduced in section 2.5 both the number of fibers N and the effective spring constant β are parameters that can be adjusted. For the equal and local load sharing models the only adjustable parameter is the number of fibers N. All the models can use different threshold distributions as well, but the only threshold distribution used here is $P(\chi) = \chi/0.001$. As mentioned previously the results are primarily based on 500 samples for system size $N = 50^2$, but the strain curve is also given for $N = 20^2$ and it will be based on 3125 samples. The different values of β used are 10^1, 10^0, 10^{-1}, 10^{-2}, 10^{-3}, 10^{-4} and 10^{-6} in ascending order of stiffness.

4.2.1 Strain Curve

The strain curves for the different values of β for $N = 50^2$ and $N = 20^2$ are presented in figures 4.4 and 4.5 respectively. Both figures has the fraction of broken fibers k/N on the

horizontal axis, making it easier to compare values for the same fraction of broken fibers. The vertical axis is $2\alpha/\beta$, which was argued to be equivalent to σ/κ for the equal load sharing model in section 2.5.2. In figure 4.4 the strain curve for the different values of β are presented in plots containing the strain curve for one value of β each, which makes it easier to see all the details of each curve. Figure 4.5 shows the strain curves for the same values of β as in figure 4.4, but the system size is only $N = 20^2$.

4.2.2 Breaking Order and Cluster Statistics

An essential part in understanding how a new model behaves is to look at which fibers break when and how the clusters of broken fibers develop. How the breaking process unfolds for different systems can be seen from looking at snapshots of the system for a random realisation. Figure 4.6 shows four snapshots for a chosen realisation of a system for three different values of β. The values for β are 1, 10^{-2} and 10^{-6}, and each snapshot in the figure is for the same number of broken fibers k for all the three different values of β. Yellow represents the intact fibers while black represents the broken fibers. Each column only contains one value of β, and they are in descending order of β from left to right.

From figure 4.6 the development of the largest cluster and of the number of clusters can be seen qualitatively. In figures 4.7 and 4.8 these quantities are plotted for all parts of the breaking process. Figure 4.7 shows the average size of the largest clutser in the system S_{MAX} divided by the number of fiber N for all points in the breaking process. The red line in the figure is the result for the equal load sharing model, and it is inserted in the same plot in order to have a curve of reference. The same has been done for the average number of clusters N_d in figure 4.8 for the same systems and realisations. All results are for systems consisting of $N = 50^2$ fibers and the averaging use 500 samples.

4.2.3 Consecutively Broken Fibers

The average distance between two consecutively breaking fibers, $\langle \Delta r^2 \rangle^{1/2}$, for the whole breaking process is presented in figure 4.9. Each plot is for a different value of β and given by the black circles. The theoretical result for the equal load sharing model, given by (2.8), is plotted as a line of reference for the systems, which have $N = L^2 = 50^2$ fibers.

4.2.4 Burst Distribution

The burst distributions $D(\Delta)$ for all the different values of β are shown in figure 4.10. In order for the plot to have a common starting point for all the burst distributions the ratio $D(\Delta)/D(1)$ is plotted for all values of β. The equal load sharing model has a theoretical burst distribution following the power law in (2.9) with exponent $\xi = 5/2$ in the large system limit. This power law is plotted on top in figure 4.10 with a manually fitted value of C in (2.9), and will be used as a line of reference to compare the results from the bridge model against.

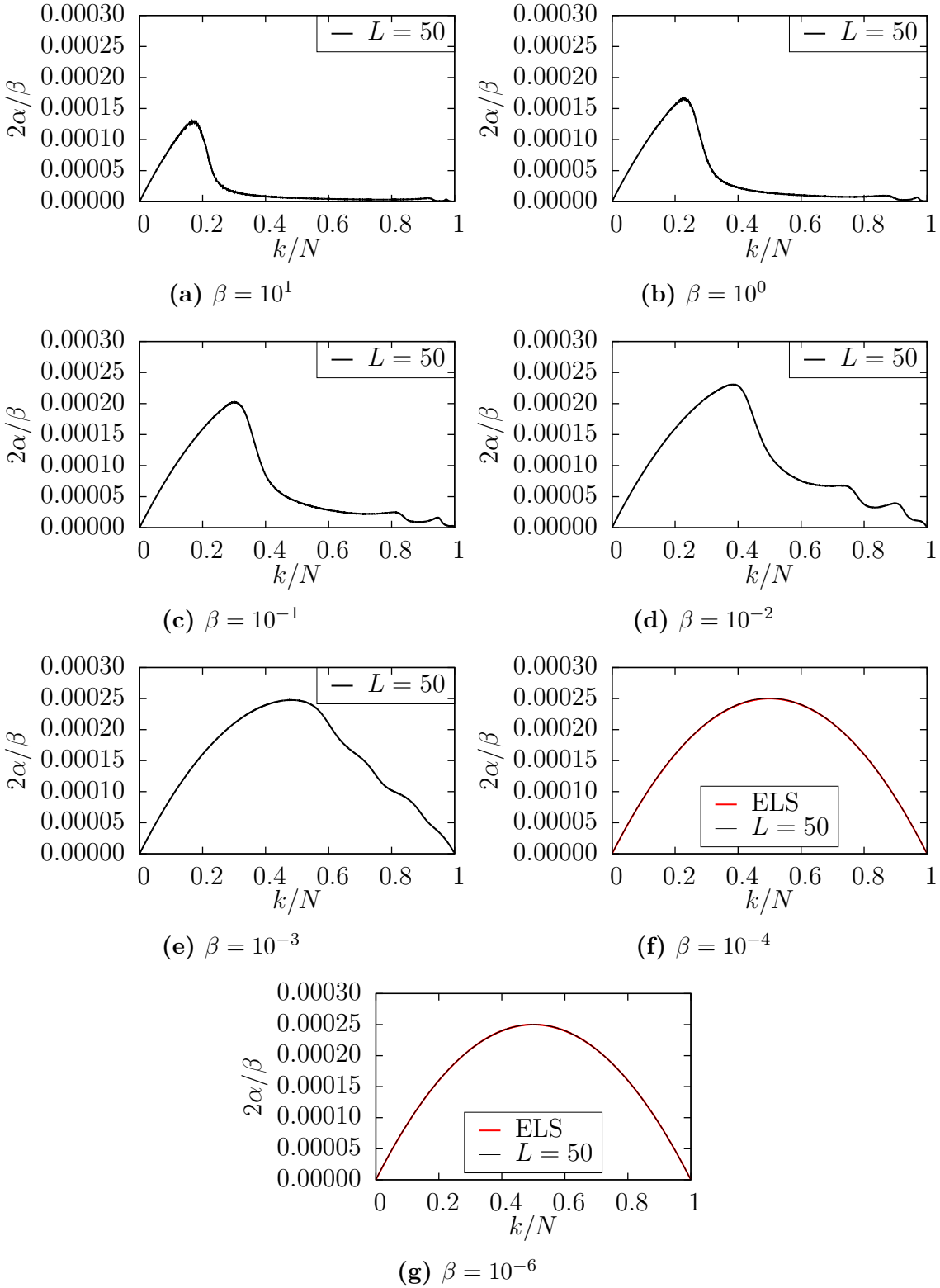

(a) $\beta = 10^{1}$ **(b)** $\beta = 10^{0}$

(c) $\beta = 10^{-1}$ **(d)** $\beta = 10^{-2}$

(e) $\beta = 10^{-3}$ **(f)** $\beta = 10^{-4}$

(g) $\beta = 10^{-6}$

Figure 4.4: The figure shows the strain curves for the two dimensional bridge model for $N = 50^2$ fibers. Each plot is for a different value of β, but all of them are based on 500 samples. The largest β-value is the the softest system and the smallest value is the stiffest system.

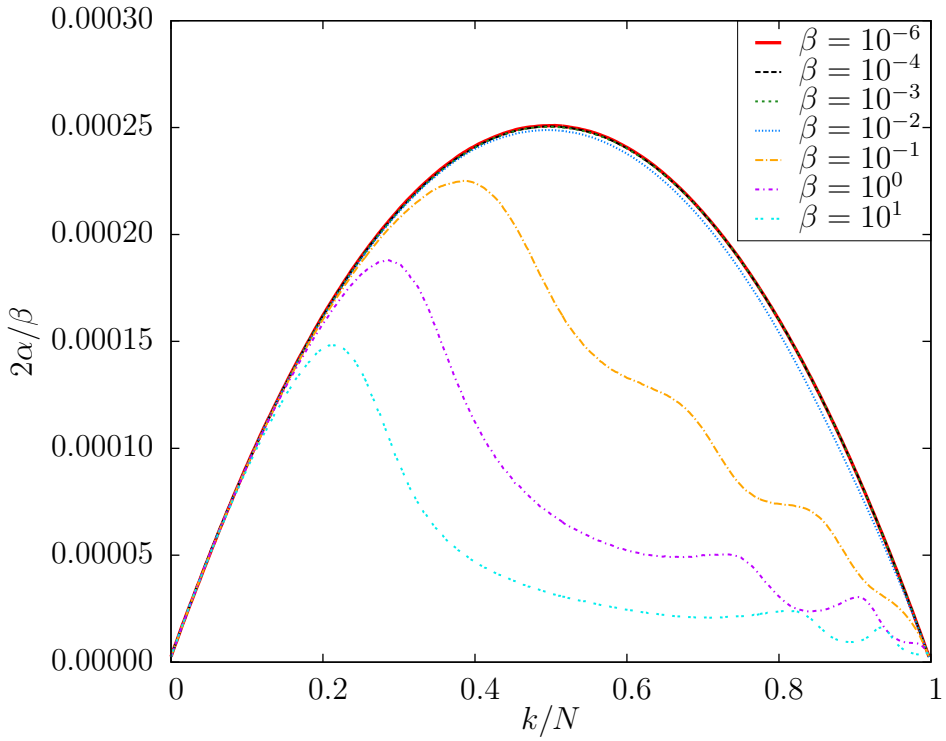

Figure 4.5: The figure shows the strain curves for the two dimensional bridge model for $N = 20^2$ fibers. Each curve is for a different value of β, but all of them are based on 3125 samples. The largest β-value is the the softest system and the smallest value is the stiffest system.

4.2.5 Force Distribution

There are no easy rules for how the force from a failed fiber is redistributed to the still intact fibers in the bridge model, unlike the equal and local load sharing models. Figures 4.11 and 4.12 show the end position $d_{i,j} = -\chi$ of all fibers when the middle fiber is broken. The systems consists of $N = 50^2$ fibers and the broken fiber is at location $(x, y) = (25, 25)$. The fibers are not included in the figure, it is only the extension χ of the fibers, which is directly proportional to the force, that is of interest. The lower the point is in the figure the greater the extension, with the only exception being the lowest point. That is the location of the broken fiber and thus no fiber is extended at that position, meaning the lowest point only represents the intersection between the cables for this point. The softest and stiffest systems are shown in figure 4.11 and the systems in between are shown in figure 4.12.

In both figures the value for α is chosen to be equal to β. With this combination of α and β, fibers which experience no extra load from the broken fiber will have an extension $\chi = -d_{i,j} = 2$. In the extreme limit of equal load sharing all fibers will have an extension of $\chi = -d_{i,j} = 2 + 8.0 \cdot 10^{-4}$, which can be seen from the expression in (2.41).

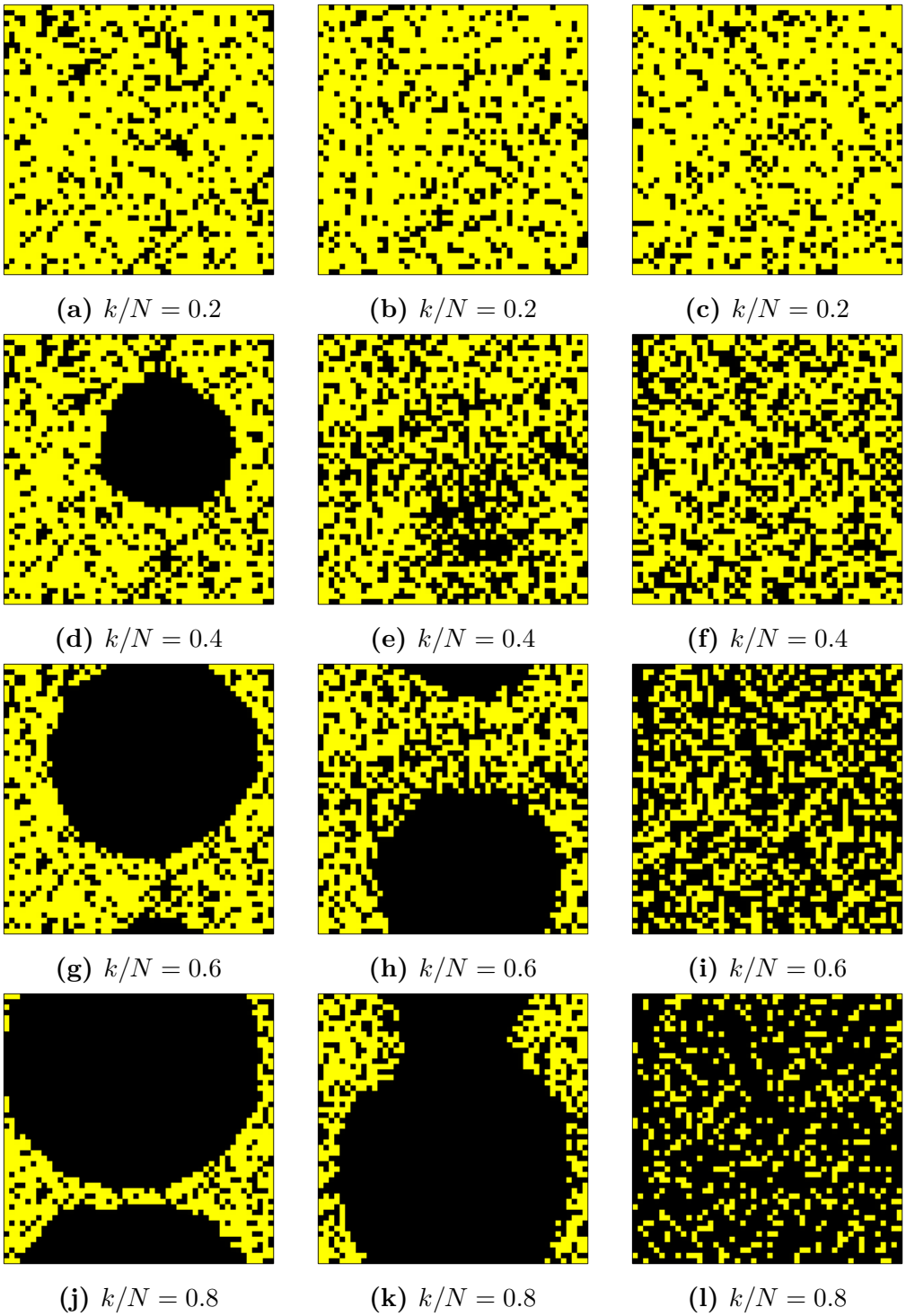

(a) $k/N = 0.2$ **(b)** $k/N = 0.2$ **(c)** $k/N = 0.2$

(d) $k/N = 0.4$ **(e)** $k/N = 0.4$ **(f)** $k/N = 0.4$

(g) $k/N = 0.6$ **(h)** $k/N = 0.6$ **(i)** $k/N = 0.6$

(j) $k/N = 0.8$ **(k)** $k/N = 0.8$ **(l)** $k/N = 0.8$

Figure 4.6: The figure shows which fibers are broken, marked in black, and which are not, marked in yellow, at a given point in the breaking process for a random realisation for three different values of β. The left column is for $\beta = 1$, the center column is for $\beta = 10^{-2}$ and the right column is for $\beta = 10^{-6}$. The number of fibers is $N = 50^2$ for all systems.

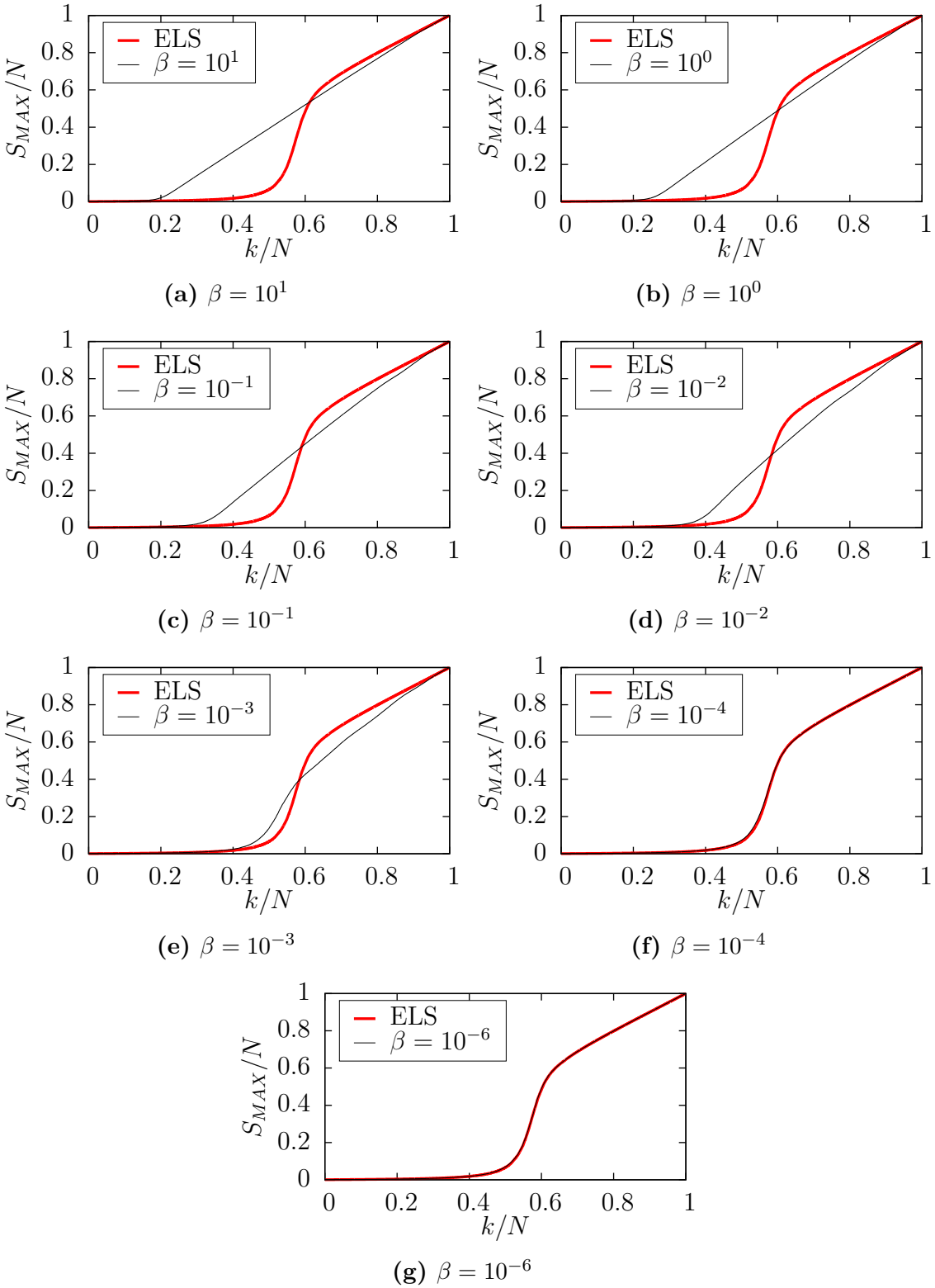

(a) $\beta = 10^{1}$

(b) $\beta = 10^{0}$

(c) $\beta = 10^{-1}$

(d) $\beta = 10^{-2}$

(e) $\beta = 10^{-3}$

(f) $\beta = 10^{-4}$

(g) $\beta = 10^{-6}$

Figure 4.7: The figure shows the average size of the largest cluster S_{MAX} for the two dimensional bridge model, black, and for the equal load sharing model, red. Each plot is for a different value of β, but the result for the equal load sharing model is the same in all plots and used as curve of reference. The results are based on 500 samples for system size $N = 50^2$.

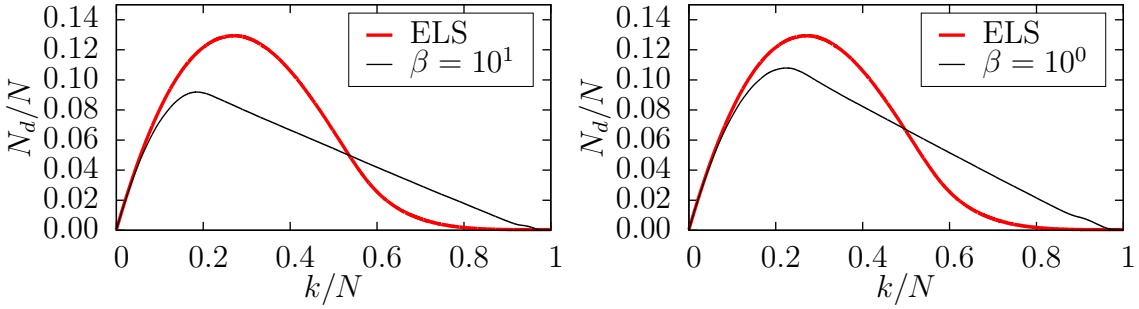

(a) $\beta = 10^{1}$

(b) $\beta = 10^{0}$

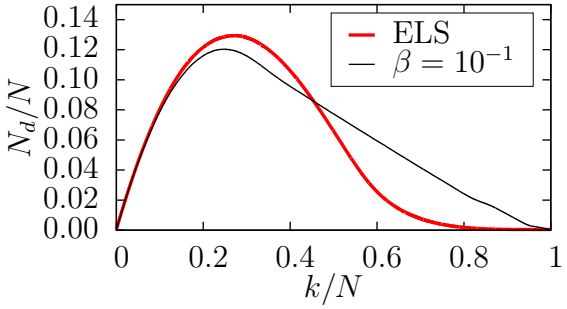

(c) $\beta = 10^{-1}$

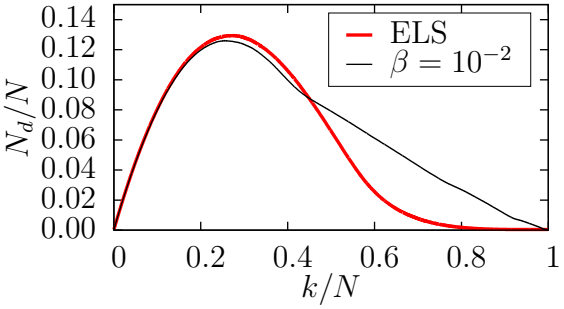

(d) $\beta = 10^{-2}$

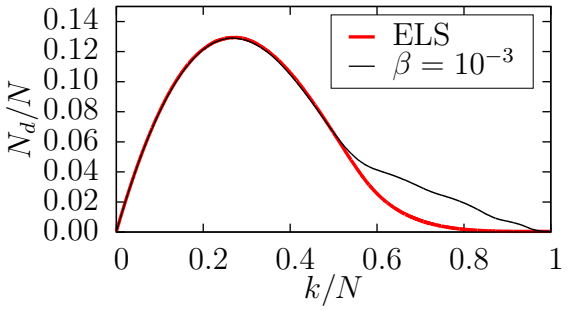

(e) $\beta = 10^{-3}$

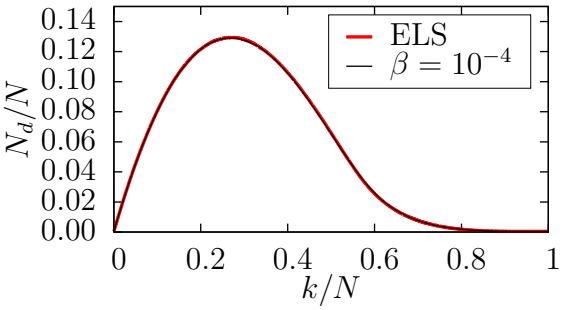

(f) $\beta = 10^{-4}$

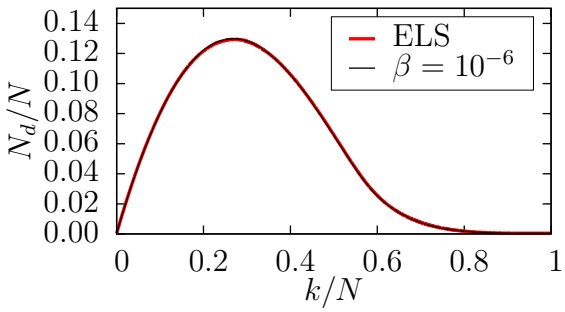

(g) $\beta = 10^{-6}$

Figure 4.8: The figure shows the average number of clusters N_d for the two dimensional bridge model, black, and the equal load sharing model, red. Each plot is for a different value of β, but the result for the equal load sharing model is the same in all plots and used as a curve of reference. The results are based on 500 samples for system size $N = 50^2$.

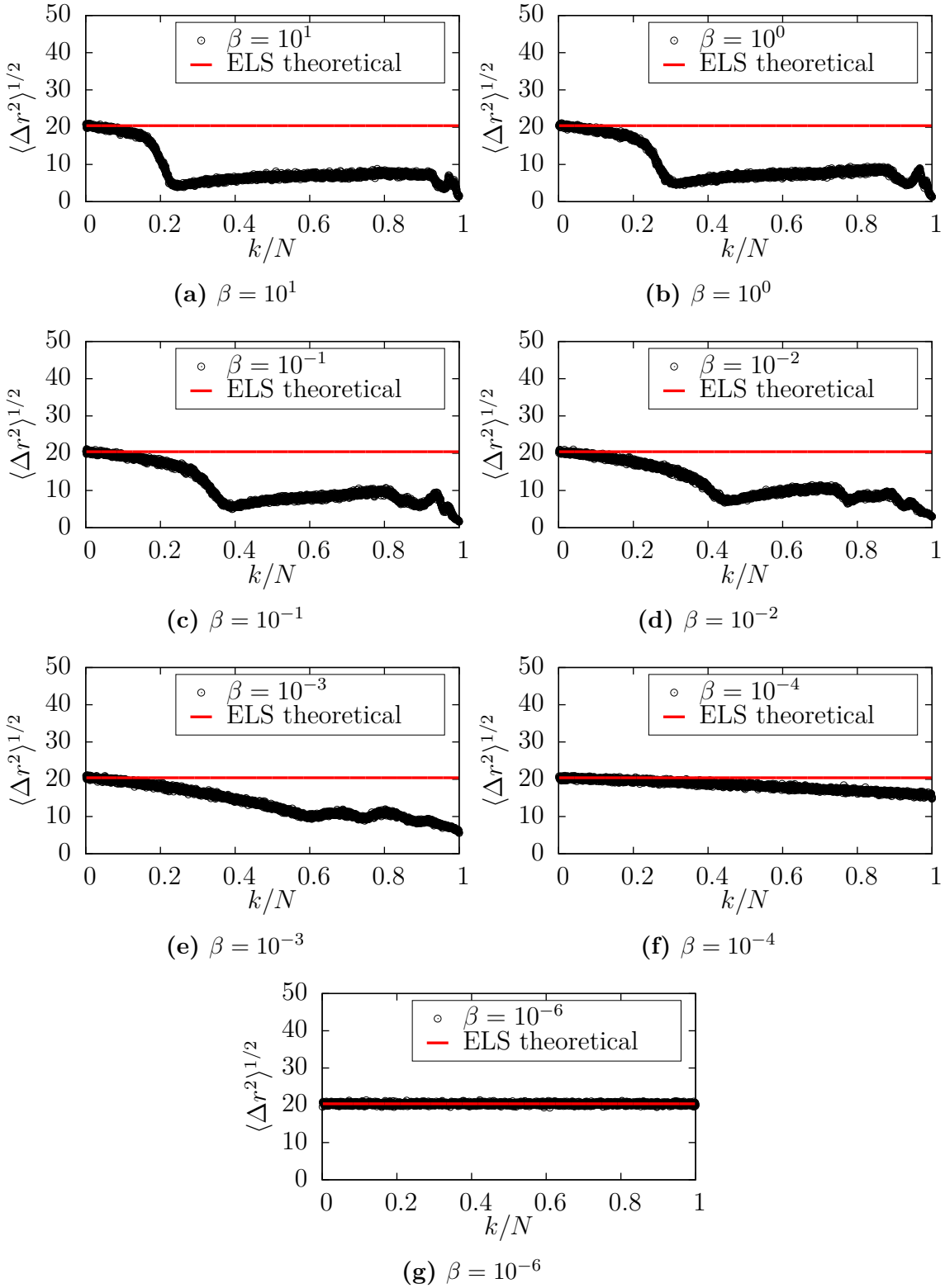

(a) $\beta = 10^{1}$

(b) $\beta = 10^{0}$

(c) $\beta = 10^{-1}$

(d) $\beta = 10^{-2}$

(e) $\beta = 10^{-3}$

(f) $\beta = 10^{-4}$

(g) $\beta = 10^{-6}$

Figure 4.9: The figure shows the average distance $\langle \Delta r^2 \rangle^{1/2}$ between fibers breaking consecutively plotted against the fraction of fibers broken k/N. The red line is the theoretical result for the equal load sharing model given by (2.8) using the system size $L = 50$.

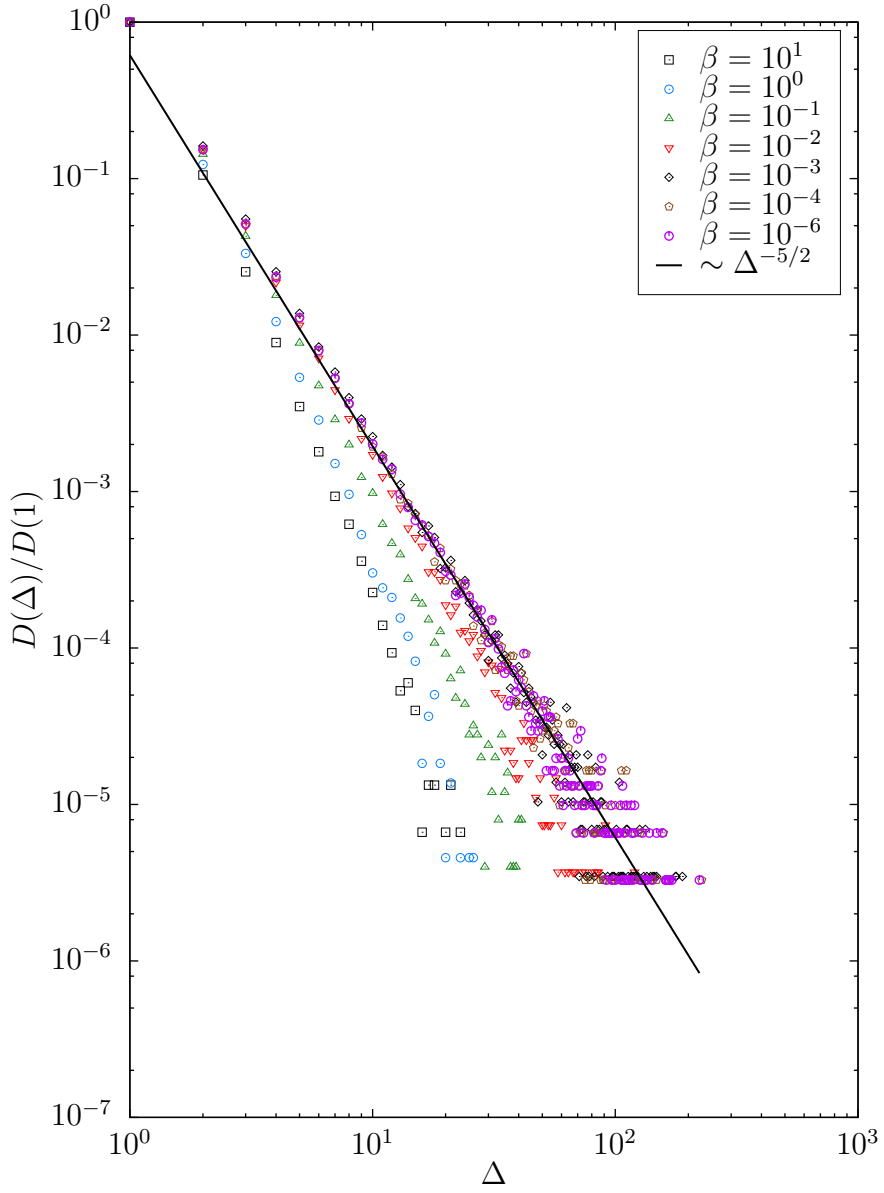

Figure 4.10: The figure shows the burst distribution for the two dimensional bridge model for different values of β. Each value is represented by its own shape and color of the points, and each of the burst distributions $D(\Delta)$ is plotted as $D(\Delta)/D(1)$ in order to have a common starting point. All the burst distributions are for systems with $N = 50^2$ fibers, and the values are the average of 500 samples. The black line in the figure is the power law in (2.9) with exponent $\xi = 5/2$, where the constant is C is chosen manually. The power law is the theoretical burst distribution for the equal load sharing model in the large system limit.

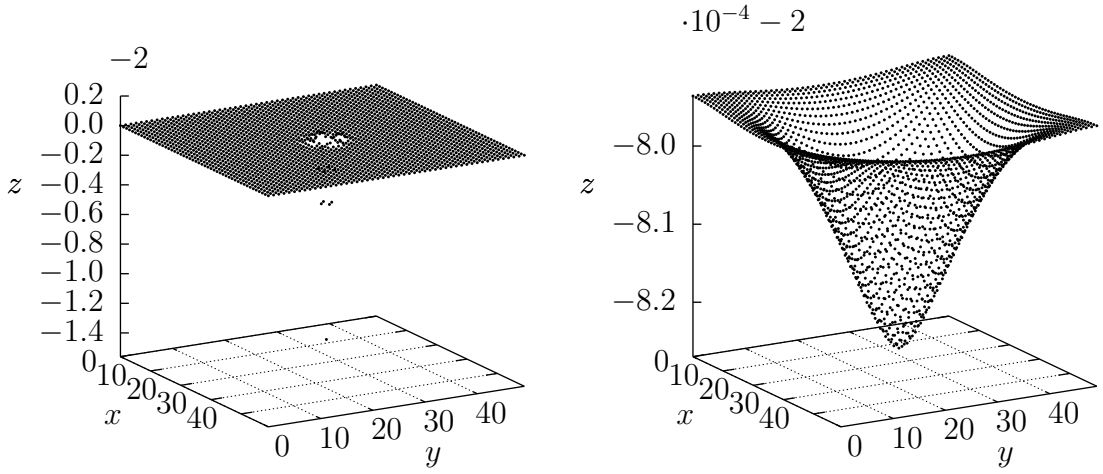

(a) $\beta = 10^1$ **(b)** $\beta = 10^{-6}$

Figure 4.11: The figure shows the position of each intersection between the cables, $d_{i,j} = -\chi$, for the softest, $\beta = 10^1$, and stiffest, $\beta = 10^{-6}$, systems simulated when the middle fiber is broken. Both systems are of size $N = 50^2$ and the middle fiber is the only broken fiber. The lowest point is the one corresponding to the broken fiber, and is thus not subject to force from a fiber. Note the scaling and shift of the vertical axis in each plot.

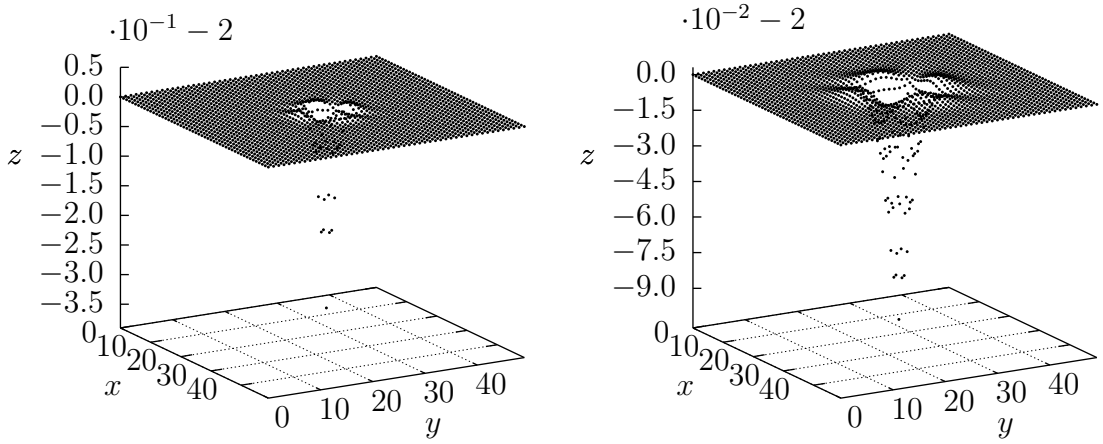

(a) $\beta = 10^0$

(b) $\beta = 10^{-1}$

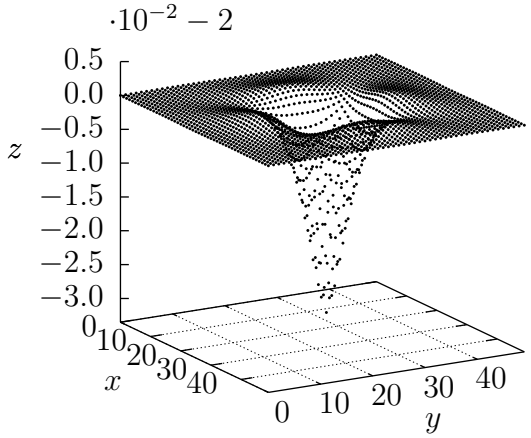

(c) $\beta = 10^{-2}$

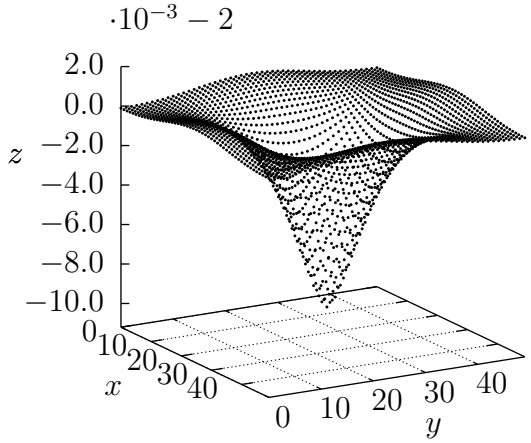

(d) $\beta = 10^{-3}$

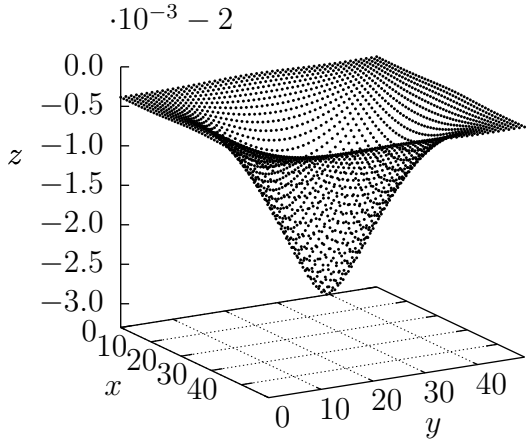

(e) $\beta = 10^{-4}$

Figure 4.12: The figure shows the position of each intersection between the cables, $d_{i,j} = -\chi$, for the systems betweem the softest and stiffest simulated when the middle fiber is broken. All systems are of size $N = 50^2$ and the middle fiber is the only broken fiber. The lowest point is the one corresponding to the broken fiber, and is thus not subject to force from a fiber. Note the scaling and shift of the vertical axis in each plot.

5 Discussion

In this chapter the results in chapter 4 will be discussed and compared. The results for the equal load sharing model are briefly discussed in section 5.1 before the results for the bridge model are discussed in section 5.2. The results for the bridge model will be compared to the results for the equal load sharing model from chapter 4, and to the local load sharing model and the soft clamp model where it is natural and possible.

5.1 The Equal Load Sharing Model

The equal load sharing model with the uniform threshold distribution $P(\chi) = \chi/\chi_r$ has several analytical results, which are presented in section 2.2. One of these results are the strain curve given by (2.7), which is plotted in figure 4.1. In the same figure the strain curve based 500 samples for a system of $N = 50^2$ fibers is present, and it is consistent with the analytical result. The derivation of (2.7) used the assumption of large system size N, and the expression is the average value for the statistically uniform threshold distribution. Thus, the overlap of the curves in figure 4.1 suggests the number of samples and system size is sufficient to get the expected average result for the large system limit.

Figure 4.2 shows the averaged distance between two consecutively breaking fibers, $\langle \Delta r^2 \rangle^{1/2}$, for each step in the simulations. The theoretical result in (2.8) for $L = 50$ is plotted as well, and it is easy to see the average value from the simulations is in compliance with the theoretical result. This means the average length betweem two consecutively breaking fibers is the same as the average distance between two points in the system. This is something that is a property common for all threshold distributions $P(\chi)$ in the equal load sharing model as long as the distribution does not depend on the position of the fibers. It is thus a good indicator for wether a model is an equal load sharing model or not.

The theoretical burst distribution for the equal load sharing model in the large system limit is the power law (2.9) with exponent $\xi = 5/2$. In figure 4.3 this is plotted in red together with the results from the simulations in black. The constant C in (2.9) was chosen manually to fit the simulated result. The smallest bursts in the burst size distribution $D(\Delta)$ does not follow the power law line, due to the small size of the bursts combined with the use of the Stirling approximation [12] in the derivation of (2.9) which require large bursts. For bursts larger than $\Delta \approx 10$ the result is consistent with the theoretical power law, supporting the notion that the implementation of the model is correct. The burst distribution fans out

for the largest burst sizes Δ, due to the limited number of samples. For the largest bursts there are only a few of each size in the 500 samples, meaning the statistics are bad.

The results for the equal load sharing model are all consistent with theory and established results. The figures and results from the simulations will be a good reference when looking at the two dimensional bridge model in section 5.2. When results are based on averages from a limited number of realisations the quality of the results depend on the number of samples and system size. This is why the number of samples and system sizes for the equal load sharing model and the bridge model was chosen to be same.

5.2 The Bridge Model

The fiber bundle bridge model has some very interesting results, and the qualitative behaviour of the model will be discussed in this section. For the stiffest systems the behaviour will be compared to the already established results of the equal load sharing model. How the force on each fiber in a system with a single broken fiber will be discussed in section 5.2.1 before describing the strain curves in section 5.2.2. When discussing the strain curves there will also be a description of the qualtitative behaviour of the breaking process, which will be covered in greater detail in section 5.2.3. The average distance between fibers breaking and the burst size distribution will be covered last, in section (5.2.4) and 5.2.5 respectively.

5.2.1 Force Distribution

How the force is redistributed when a fiber breaks is one of the main properties distinguishing different fiber bundle models. In the equal load sharing model the force is divided equally among all remaining fibers, as the name suggests, and in the local load sharing model the fraction of the total force previously carried by the failed fibers in a hole is divided equally between intact fibers in the perimeter of the hole. These two approaches are the extreme opposites of each other and give rise to different behaviour. The rules for the equal and local load sharing models are very simple, and the change in fraction of force carried by the fibers when a fiber breaks can theoretically be done by hand for all system sizes. For the bridge model there are no such easy rules, the matrix problem in (2.34) has to be solved in order to find the forces each time a fiber breaks.

Figures 4.11 and 4.12 shows a system of $N = 50^2$ fibers with the middle fiber, located at $(i, j) = (25, 25)$, broken for different values of β. For all systems the value of α was chosen to be equal to β, resulting in an extension of $\chi = -d_{i,j} = 2$ when a fiber is not subjected to an increased fraction of the total force. For the system in the figures, which consists of $N = 50^2$ and has $k = 1$ broken fibers, the extension will be $\chi = 2 + 8.0 \cdot 10^{-4}$ if the total force is divided equally between all intact fibers. For the softest system, $\beta = 10$, in figure 4.11a the effective range of interaction is very small. Only a few fibers in close vicinity of the broken fibers experience an increased fraction of the total force. It is also possible to see the affected fibers are not only the four nearest neighbours, as it would have been in the extreme case of equal load sharing. For the bridge model there is a finite range of interaction greater than just the nearest neighbours.

Figure 4.11b is the extension of the fibers for the stiffest system used, $\beta = 10^{-6}$. All the intact fibers in the system are extended beyond $\chi = 2$, which is the extension of a fiber experiencing no extra load due to the broken fiber. The extension of the fibers are close to the equal load sharing value of $\chi = -d_{i,j} = 2 + 8.0 \cdot 10^{-4}$, but there are some slight variation between fibers. The variation is very small compared to the total extension of the fibers, making it clear the effective range of interaction is large enough to span the system size, affecting all fibers. If one fiber breaks all fibers will experience an increase in fraction of total force experiences, and the difference in extension between the most and least extended fibers is very small relative the total extension for $N = 50^2$ and $\beta = 10^{-6}$.

The systems in between $\beta = 10$ and $\beta = 10^{-6}$ are presented in figure 4.12. The effective range of interaction is small for the softer systems, but it increase gradually as the systems become stiffer and stiffer when the value of β decrease. For $\beta = 1$, shown in figure 4.12a, the fibers closest to the broken fiber are extended the most and the extra extension of fibers rapidly decrease as the distance to the broken fiber increase. Sufficiently far away from the broken fiber some fibers are actually extended less than when all fibers were intact due to the bending ridigity of the cables. When the system gradually becomes stiffer in figures 4.12b and 4.12c the pattern of fibers experiencing an increased or decreased fraction of total force has the same basic shape as in figure 4.12a, but the affected area is larger the stiffer the system is. The cables forming the model has a bending rigidity B, and when a cable is at an angle to the (x, y)-plane due to a nearby hole there is a finite distance needed for the cable to bend back to horizontal position. Since the the total force is held constant, the bending of the cables will cause some fibers to be extended less than when the fiber in question was not broken. In both figure 4.12b and figure 4.12c the fibers at the boundary of the figure is not noticably affected by the broken fibers, meaning the effective range of interaction is not large enough to span the whole system yet.

Figure 4.12d and 4.12e show the effective range of interaction starting to be large enough for all fibers to be affected by the broken fiber in the middle. As the value of β gets lower, the difference between the extension of the fibers which is extended the most and of the fibers extended the least decrease. This is highlighted by the smallest relative difference in height occurs for the the lowest value of β used in the simulations, with a relative difference of the order 10^{-4} for figure 4.11b where $\beta = 10^{-6}$.

The way the force is distributed when a single fiber is broken, shown in figure 4.11 and figure 4.12, suggests the model will be highly localized for the higher values of β used. For the lowest values of β on the other hand, the behaviour is closer to a mean field behaviour. In between there will be a finite range of interaction and the the effect of broken fibers have an effective range of interaction depending on the value of β.

5.2.2 Strain Curve

The strain curves for the two dimensional bridge model depends on both the system size and the value of β, as can be seen in figures 4.4 and 4.5. The lower the value for β is, the closer the strain curve is to the strain curve for the equal load sharing in figure 4.1. For the system of $N = 50^2$ in figure 4.4 the strain curve for both $\beta = 10^{-4}$ and $\beta = 10^{-6}$ are consistent with the result for the equal load sharing model, which is further evidence supporting the two

dimensional bridge model is approaching the equal load sharing model for sufficiently small values of β.

The effect of the size of the system is clear to see when comparing the strain curves for $N = 50^2$ in figure 4.4 with the strain curves for $N = 20^2$ in figure 4.5. The stiffer the system behaves the closer the strain curve is to the result for the equal load sharing and the transition is gradual, as seen in figure 4.4. For a given value of β the strain curve for the smaller system is closer to the equal load sharing model compared to the larger system, which is as expected. The effective range of interaction, measured in number of fiber spacings l, is determined by the value of β. The smaller the systems is, the sooner the effective range of interaction spans the system, effectively making it close to the equal load sharing result for larger values of β compared to larger systems. This also means as the systems get sufficiently large, the value of β resulting in equal load sharing strain curve will be too small to get the required precision to solve the matrix problem in (2.34) with 64 bit numbers on a computer. This is not a big problem for later simulations as results for equal load sharing is acquired using the much faster implementation of the equal load sharing model. The limit of stiff systems is included mostly to check the results of the model, and see when the model becomes sufficiently stiff to give the results for the equal load sharing model.

The effectively stiffer system for the same values of β when the number of fibers is decreased can also be seen in the light of the definition of β in (2.15b). For a system of a fixed physical size the number of fibers L in each direction will determine the distance between two fibers l. For a given bending rigidity B and number of fibers L in each direction the system has a given behaviour. Then the number of fibers is decreased, increasing the distance between fibers to $l \to \lambda l$ where λ is greater than one. In order to have the same value for β the bending rigidity B of the cables has to increase to $B \to \lambda^3 B$. The physical system size is the same, but bending rigidity of the cables increase as the number of fibers decrease in order to have a constant value for β, explaining the change in strain curve between figure 4.4 for $N = 50^2$ and figure 4.5 for $N = 20^2$ for the same values of β. The change in stiffness when changing the number of fibers without changing the parameter in the model is something seen in the soft clamp model as well [24]. The parameters are not the same, but both models become stiffer as the number of fibers decrease.

For the strain curves in figure 4.4 with β greater than 10^{-4} there are two bumps in the curve after the critical point k_c. The value of k/N at which these are present depends on the system size, and they occur at very specific parts of the process. From figure 4.6, which will be discussed further in section 5.2.3, it is clear that a large hole of a circular shape forms during the breaking process around the critical point $k = k_c$ and the increased extension of fibers close to the hole becomes the main breaking process. At some point in the breaking process the circular cluster of broken fibers surrounded by intact fibers will change to being a single continuous strip of broken fibers with a similar strip of intact fibers. This change has already happened in figure 4.6k, and the point of the change depends on the value of β. First the circular hole grow so large that the effective range of interaction is large enough to span the narrow strip of intact fibers separating the circular hole from being a continuous strip of broken fibers. Then the weakest fibers in this thin strip of intact fibers are broken before the stronger fibers have to be broken. The extra force required to break these strong

fibers cause the first bump in the strain curve.

The second bump in the strain curve is due to a very similar mechanism. The continuous strip of broken fibers will get a more uniform width than observed in 4.6k, and then the width will become wider. At a certain width the strip of still intact fibers will become an island of intact fibers surrounded by broken fibers. For this to happen the weakest fibers in the strip starts to break and then the stronger ones before becoming an island, causing the last bump in the strain curves. The softer the systems are the later the transition from a circular hole to a continuous strip of broken fibers will occur. This is due to the hole can be larger before the effective range of interaction is large enough to break through the strip of intact fibers separating the hole from becoming a strip of broken fibers.

Figure 4.4a shows the strain curve for $\beta = 10$, and the shape is in stark contrast to the strain curve for the two dimensional local load sharing model, which can be found in [25]. The strain curve for the local load sharing model in two dimensions is closer to the result for the equal load sharing model late in the breaking process. At which point there is one very large cluster neighbouring almost all the remaining fibers, resulting in the force on all of the neighbouring fibers to be equal due to the rules for sharing the force. This is very similar to how the force is shared in the equal load sharing model at the same point in the breaking process, resulting in approximately the same shape of the strain curves late in the breaking process. For the two dimensional bridge model in the soft regime, like $\beta = 1$, the force from a large hole is not necessarily divided equally between the intact neighbours of the hole. The shape of the hole also plays a part, which can be seen from figure 4.6 where the hole is of a circular shape and when the fibers break the circular shape is kept for $\beta = 1$. If there is a thin strip of broken fibers connected to the large circular cluster the force experienced by an intact fiber in the perimeter of the thin strip will be less than a fiber in the circular part of the perimeter. The bridge model is thus not a local load sharing model according to the definition by Harlow and Phoenix [2], even though the distribution of forces from failed fibers is a highly localized process for the softest systems.

5.2.3 Breaking Order and Cluster Statistics

For new models it is always interesting to try to get a feel for how the breaking process works for different parameters. This was done in section 4.2.2 by looking at different snapshots of the breaking process for different parameters in figure 4.6 and by plotting the average size of the largest cluster of broken fibers S_{MAX} in figure 4.7 and the average number of clusters N_d in figure 4.8.

The breaking process has already been discussed slightly when discussing the strain curve in the previous section. The softest system, $\beta = 1$, is in the left column, the next softest, $\beta = 10^{-2}$ in the middle column and the stiffest, $\beta = 10^{-6}$ is in the right column of figure 4.6. In the beginning of the breaking process there are many small clusters for all the values of β, but it can already be seen that the clusters are slightly larger for $\beta = 1$. For $k/N = 0.4$ there is already a cluster of circular shape for $\beta = 1$, and it can be seen in the subsequent snapshots that the expansion of this cluster is the driving force in the breaking process for this system. This is due to the short effective range of interaction causing a large fraction of force on the fibers close to the hole. The circular form occurs at the critical point k_c in

the simulations, and in figure 4.4b it can be seen that the critical point is before $k/N = 0.4$. In the case of $\beta = 10^{-2}$ there is still no clear, circular cluster of broken fibers at $k/N = 0.4$, but it is forming an area of few intact fibers which has been turned into a circular cluster in the next snapshot at $k/N = 0.6$. This is consistent with the critical point being around $k_c/N = 0.4$ for this combination of parameters, which is the point in the breaking process the snapshot is taken from. For the large cluster to form, and later expand, enough fibers have to be broken in order for the cables to sink sufficiently down somewhere in the system. Due to the increased effective range of interaction, dividing the increased fraction of the force between more fibers, there has to be more broken fibers in close vicinity in order for this to happen for $\beta = 10^{-2}$ compared to $\beta = 1$. In the last snapshot at $k/N = 0.8$ the circular cluster has been turned into a continuous strip of broken fibers, which will widen until the strip of still intact fibers is turned into an island of intact fibers surrounded by the broken fibers. This applies also for $\beta = 1$ and other sufficiently soft systems compared to the system size. The breaking process for $\beta = 10^{-6}$ with $N = 50^2$ fibers, is as expected for an equal load sharing model, random fibers breaking without any distinct pattern. This supports that the two dimensional bridge model with $\beta = 10^{-6}$ and $N = 50^2$ fibers is close the equal load sharing model.

The breaking process is interesting to compare to the breaking process presented by Stormo for the soft clamp model in figure 4.3 in [26]. Both models have been shown to be equivalent to the equal load sharing model when the stiffness of the system tends to inifnity, and the breaking process for both systems is consistent with this for the stiff systems. As mentioned before the soft clamp model used infinitely thick elastic plates while the bridge model effectively use a thin plate which can be bent. This is two different approaches to making a fiber bundle model, but the visual breaking process is similar for both models. In both models the process starts by breaking fibers at different locations in the system before a circular cluster of broken fibers starts to form if the system is soft enough. After this has happened the cluster starts to grow radially before the cluster of broken fibers surrounded by intact fibers change to a continuous strip of broken fibers at a later point in the process. This makes sense since both models are closer to each other in approach than the equal and local load sharing models. Both have a finite range of interaction for the soft systems, and the respons of the material will be dependent on the geometrical shape for both, examplified by the thins strip of intact fibers attached to a larg circular hole, discussed in the previous section, section 5.2.2.

The visual behaviour of the breaking process of the models is very close to each other, but it is not possible to say something certain about how it is late in the process due to different system size of the bridge model and the soft clamp model in [26] and the last snapshots end before all fibers have been broken. The system on the left hand side of figure 4.6 for $\beta = 1$ has not transitioned into a continuous strip of broken fibers at $k/N = 0.8$ while the transition has already happened at $k/N = 0.75$ for the soft system in [26]. Without running the simulations for the same system size it can not be excluded that system size has an influence on when the transition happens.

Figure 4.7 and figure 4.8 takes a closer look at the qualitative behviour which is present in figure 4.6. The first figure shows the average size of the largest cluster S_{MAX} during the

breaking process and the latter shows the average number of clusters N_d. For $\beta = 10^{-6}$ both S_{MAX} and N_d are consistent with the results for an equal load sharing system of the same number of fibers, $N = 50^2$. The results for $\beta = 10^{-4}$ are also very close, but the largest cluster S_{MAX} starts the rapid growth, at about $k/N = 0.5$, slightly before the equal load sharing result. This suggests the model is close to an equal load sharing model, but not close enough for the results to be indistinguishable. For the equal load sharing model the largest cluster is small early in the process since it always breaks the weakest fiber, giving a lot of clusters of small size. As the breaking process goes on the number of possibilities for making new clusters decrease, making the largest cluster slightly larger. At some point all the small clusters are merged into a large cluster while only a small fraction of the fibers in the system are breaking, resulting in the very steep part of the curve in figure 4.7. in the steepest area in figure 4.7. Afterwards almost all new fibers breaking become part of the spanning cluster and the largest cluster grows with approximately one fiber for each fiber breaking after $k/N \approx 0.7$.

For the softer systems the number of clusters will increase rapidly at the start due to the lack of large areas of broken fibers at the start, and thus the largest cluster size is kept small. After the critical point k_c there will only be one large cluster growing radially. As can be seen in figure 4.7 the size of the largest cluster grows with more than one fiber per fiber breaking at this point. This is caused by the relatively large number of small clusters which are merged with the large circular cluster of broken fibers. For the softest systems the growth is almost linear after the large cluster has started to grow, which is reflected in the gradual decrease in the average number of clusters in figure 4.8. As the system becomes stiffer the critical point k_c is later in the breaking process and the formation of the circular cluster of broken fibers is forming later, causing S_{MAX} and N_d to be closer to the results for the equal load sharing model. For $\beta = 10^{-3}$ the average largest cluster size is low before suddenly growing fast. Before it contains almost all the broken fibers in the system, as the equal load sharing model does, it starts merging with small clusters like the softer systems. This is supported by the number of clusters in figure 4.8e, which follows the equal load sharing curve closely before it suddenly decrease much slower.

For soft systems a large circular cluster of broken fibers occur early in the breaking process which will expand as more fibers break. This causes an almost linear increase in the average size of the largest cluster S_{MAX} and almost linear decrease in the average number of clusters N_d. As the systems gets stiffer the large circular cluster forms later and the largest cluster size stays low for a longer period of the breaking process. As the stiffness of the system becomes sufficiently large there is no circular cluster forming and the development of the average size of the largest cluster S_{MAX} and the average number of clusters N_d become consistent with the development for the equal load sharing model. Visually the breaking process for the soft and stiff systems are similar to the breaking process for soft clamp model based on the snapshots of the systems presented in [26].

5.2.4 Consecutively Broken Fibers

The average distance between two fibers breaking consectuively, $\langle \Delta r^2 \rangle^{1/2}$, is a great measure to see if a model is consistent with the equal load sharing model or not. If it is not consistent it is also of interest to see how the distance change for different parts of the breaking process for different values of β. $\langle \Delta r^2 \rangle^{1/2}$ is plotted for different values of β for system size $N = 50^2$ in figure 4.9. The red line in the plots are the theoretical result for the equal load sharing model.

It is clear to see the average distance between two consecutively breaking fibers is consistent with the equal load sharing model for $\beta = 10^{-6}$ and $N = 50^2$. The result can be seen in figure 4.9g, and the values and the width of the line is consistent with the result for the equal load sharing model in figure 4.2. None of the other values for β with system size $N = 50^2$ shows this behaviour, which means $\beta = 10^{-4}$ and higher values are not equivalent to the equal load sharing model for this system size. In the case of $\beta = 10^{-4}$ the strain curve in figure 4.4f is consistent with the strain curve for the equal load sharing model in figure 4.1, suggesting it is close to the equal load sharing model. But the fact that the average distance between two consecutively breaking fibers is decreasing as the breaking process proceeds in figure 4.9f means the model can not be equivalent to the equal load sharing model. When the result does not have the value given by (2.8) the location of the next fiber to break is no longer equally likely to be at all possible locations in the system, which should be the case for the equal load sharing model. Both figure 4.9f and figure 4.9g has the same qualitative shape as the two stiffest systems used by Stormo for the soft clamp model in figure 4.2 in [26]. This suggests the breaking behaviour for the stiffest systems used is qualitatively equal. For the stiffest system the result is consistent with the equal load sharing model for both models, as expected for stiff systems.

For the softer systems the average distance between two consecutively breaking fibers is not constant during the breaking process. Right at the start of the breaking process for the systems in figure 4.9 the distance begins at the theoretical value for equal load sharing in (2.8). At the start of the breaking process there are some very weak fibers compared to others, and these are the ones breaking first, even for the soft systems. When only one fiber is broken the relative increase in extension even for $\beta = 10$ is small compared to the total extension of the fibers not experiencing an increased fraction of the force. Thus, it is usually the next weakest fiber to break, the same as in the equal load sharing model for the same step. This makes the average distance $\langle \Delta r^2 \rangle^{1/2}$ consistent with the result for the equal load sharing model in the very beginning of the breaking process. Soon after the average distance is decreasing as the broken fibers cause an increase in force for the surrounding fibers, and fibers are more likely to break close to the previously broken fiber compared to the equal load sharing model. For the softest systems used, like $\beta = 1$ in figure 4.9b, $\langle \Delta r^2 \rangle^{1/2}$ decrease rapidly as the large, circular hole is created. From then on the fibers break radially from the hole, slowly increasing the average distance between two consecutively breaking fibers as the size of the hole increase. The effects on the end is due to the previously discussed transition from a hole of broken fibers surrounded by intact fibers to a continuous strip of broken fibers to only an island of intact fibers surrounded by broken fibers. This effect is present for all values of β higher than 10^{-4} in figure 4.9, even though the length of the different regions are

different due to the difference in bending stiffness. For the softest systems the creation of the large circular cluster at the critical point k_c occurs earlier than for the stiffer systems, as illustrated in figure 4.4, and due to the short range of interaction it can be larger than for stiffer systems before the circular hole becomes a strip of broken fibers.

For the soft systems the comparison to the average distance between consecutively breaking fibers for the soft clamp model presented in [26] is not as straight forward as it was for the stiffer systems. The largest problem is the discrepancy in the system size, with $N = 50^2$ in figure 4.9 for the bridge model and $N = 128^2$ for the soft clamp model in figure 4.2 in [26]. Both models starts at the value for the equal load sharing model, but is decreasing slowly right from the start. Around the critical point the average distance between consecutively failing fibers is reduced much faster than before the critical point for both models as well. After the critical point it become harder to compare the models due to the difference in size. Both models can be seen to have a drastically shorter average distance betewen consecutively breaking fibers compared to the value for the equal load sharing model, giving a highly localized behaviour of the models. In the bridge model there are some very distinct increases and decreases in the distance late in the simulation, as seen in figure 4.9. There are some tendencies to such behaviour for the softer systems for the softest systems in the soft clamp model as well, but not as distinct, which may be because of the system size as well. Equal number of realisations for the same system size of both models should be simulated in order to make a better comparison.

5.2.5 Burst Distribution

The burst distribution for different values of β for $N = 50^2$ was presented in figure 4.10 together with the power law in (2.9) with exponent $\xi = 5/2$. The constant C was manullay chosen in order to get a good overlap with the data for the stiffest system, and it is only used as a reference.

For the three stiffest systems, $\beta = 10^{-6}$, $\beta = 10^{-4}$ and $\beta = 10^{-3}$, it is hard to see any difference in the burst distributions, and the little difference there is may be caused by statistical variations for the large systems. The data is based on 500 samples of a system with $N = 50^2$ fibers for each value of β, and for the largest burst sizes Δ there is only a few bursts of the size across all samples. The lowest value for $D(\Delta)$ for each value of β in (4.10) corresponds to only one burst of the size in question in all the samples. For bursts of size larger than $\Delta \approx 10$ the results are consistent with the power law in (2.9) with exponent $\xi = 5/2$. The results seem consistent with the results from the equal load sharing model in figure 4.3, which is known to follow a power law for sufficiently large systems and bursts. Due to the limited number of samples and limited system size, it is very hard to notice any possible subtle differences from the equal load sharing results in figure 4.3. The distribution for the bursts smaller than $\Delta \approx 10$ falls of quicker than plotted power law line in figure 4.10, just as it is does for the equal load sharing model in figure 4.3. In the derivation of the power law in (2.9) the Stirling approximation was used for the burst size Δ, and that is only a good approximation for sufficiently large bursts.

The burst size distribution for $\beta = 10^{-2}$ and larger falls off quicker than the power law in (2.9) with $\xi = 5/2$. The larger the value of β the faster the burst distribution falls off for the

larger bursts. For $\beta = 10^1$ $\beta = 10^0$ even the largest bursts are under $\Delta = 30$, which is small compared to the largest burst for $\beta = 10^{-6}$ which is larger than $\Delta = 200$. The amount of data available at this point in time is not enough to determine wether the burst distribution for these softer systems is exponential, a power law or something else. For $\beta = 10^1$ and $\beta = 10^0$ $D(\Delta)$ seems to fall of quicker than a power law, but for the other values it is even harder to say something about it. To really find out the form of the burst distribution for the two dimensional bridge model vast amount of data is needed, which is unfortunately not possible to get within a reasonable time frame yet.

6 Conclusion

The two dimensional fiber bundle bridge model has been derived and introduced in this thesis. The model is based on the one dimensional fiber bundle bridge model, which is independent of history and has an effective range of interaction. The two dimensional model has inherited these traits and has two parameters, the number of fibers N and β which is directly proportional to the spring constant κ divided by the bending rigidity of the cables in the model B. For a given system size the value of β determines the stiffness of the system, with low values being stiff systems and high values being soft systems. When the system size is reduced while keeping β constant the system behaves as a stiffer system compared to the system of original size.

In the limit of cables of infinite bending rigidity B the model is shown to be analytically equivalent to the equal load sharing model, which all results support. The strain curve, average size of the largest cluster S_{MAX}, average number of clusters N_d, average distance between two consecutively breaking fibers $\langle \Delta r^2 \rangle^{1/2}$ and burst size distribution $D(\Delta)$ are all consistent with the results obtained for the equal load sharing model for the same system size.

For the softest systems, with the highest values of β, the model does not behave like the local load sharing model, even though the one dimensional bridge model was a local load sharing model for soft systems. The behaviour is highly localized around clusters of broken fibers in the simulation, but the force previously carried by the broken fibers in the clusters is not divided equally between the nearest neighbours of the clusters. This is due to the extra dimension making it possible for a cluster of broken fibers to have more than two intact neighbours, giving more intricate cluster shapes. When a sufficient amount of fibers are broken a circular cluster of broken fibers is formed sufficiently soft systems and the fibers breaking afterwards are in close vicinity of this cluster.

The formation of a circular cluster is similar to the behaviour of the soft clamp model, which also develop a circular cluster for soft systems. This causes the average distance between consecutively breaking fibers to decrease drastically for both models. When reducing the number of fibers, while keeping the physical system size and the dimensionless parameter adjusting the stiffness of each model constant, both models become effectively stiffer. The behaviour of both models seem similar, but the amount of comparable data available at the time of writing is unfortunately insufficient to be able to do a proper analysis of the differences in the models. The soft clamp model use infinitely thick elastic plates and the bridge model represents a very thin plate with holes that can be bent, so it is expected to be some differences between the models.

The effective range of interaction is adjusted by changing the value of the effective spring constant β, and it is possible to gradually go from a very short effective range of interaction to having it span the system size. As long as the effective range of interaction is not very close to the system size, a circular cluster of broken fibers will form during the simulation and drive the breaking process afterwards. The stiffer the system the later the cluster appear, and the distance from the edge of the cluster to the fibers likely to break increase with increasing system stiffness. Qualitatively the breaking process in the bridge model and soft clamp model are similar, but there is insufficient data to make a proper comparison at the time of writing.

6.1 Suggestion for Future Work

With such a new model as the two dimensional fiber bundle bridge model the greatest limiting factor for what to do next is the imagination. In this thesis selected basic results have been produced and studied for limited number of realisations. There is a large scope for getting more data and looking at different results, threshold distributions, systems sizes and so on.

The natural continuation of this thesis would be to continue the quest for a good iterative solver, hopefully outperforming the direct solver used now by a big margin. This would make it feasible to simulate much larger systems compared to the system sizes used in this thesis. It would also make it possible to get better statistics and maybe look at the burst distribution and other quantities demanding good statistics in order to determine the behaviour.

It would also be desirable to start a systematic comparison with the soft clamp model, where both models are simulated for the same system sizes and the same number of realisations. Then the same quantities for both models could be studied for the same system sizes. This would hopefully make it possible to see where the bridge model and the soft clamp model differs, if they differ. The soft clamp model consists of infinitely thick plates while the bridge model is effectively a very thin bendable plate with holes, so it would be expected the results differs slightly. With the combination of results available for both models at the time of writing, it is hard to pinpoint the differences.

Bibliography

[1] F. T. Peirce. "Tensile Tests for Cotton Yarns v. - "The Weakest Link" Theorems on the Strength of Long and of Composite Specimens". In: *Journal of the Textile Institute Transactions* 17 (7 1926), pp. 355–368.

[2] D. G. Harlow and S. L. Phoenix. "The Chain-of-Bundles Probability Model For the Strength of Fibrous Materials I: Analysis and Conjectures". In: *J. Composite Materials* 12 (Apr. 1978), pp. 195–214.

[3] N. Pollen and A. Simon. "Estimating the mechanical effects of riparian vegetation on stream bank stability using a fiber bundle model". In: *Water Resources Research* 41.7 (2005). W07025, n/a–n/a. ISSN: 1944-7973. DOI: 10.1029/2004WR003801. URL: http://dx.doi.org/10.1029/2004WR003801.

[4] I. Reiweger et al. "Modelling snow failure with a fibre bundle model". In: *Journal of Glaciology* 55.194 (2009-12-01T00:00:00), pp. 997–1002. DOI: doi:10.3189/002214309790794869. URL: http://www.ingentaconnect.com/content/igsoc/jog/2009/00000055/00000194/art00005.

[5] B. K. Chakrabarti. "A fiber bundle model of traffic jams". In: *Physica A: Statistical Mechanics and its Applications* 372.1 (2006), pp. 162–166. ISSN: 0378-4371. DOI: http://dx.doi.org/10.1016/j.physa.2006.05.003. URL: http://www.sciencedirect.com/science/article/pii/S0378437106005838.

[6] G. G. Batrouni, A. Hansen, and J. Schmittbuhl. "Heterogeneous interfacial failure between two elastic blocks". In: *Phys. Rev. E* 65 (3 Feb. 2002), p. 036126. DOI: 10.1103/PhysRevE.65.036126. URL: http://link.aps.org/doi/10.1103/PhysRevE.65.036126.

[7] H. T. Nygård. *The Fiber Bundle Bridge Model*. Specialization Project, Norwegian University of Science and Technology, (unpublished). 2016.

[8] A. Hansen, P. C. Hemmer, and S. Pradhan. *The Fiber Bundle Model. Modeling Failures in Materials*. 1st ed. Wiley VCH, 2015. Chap. 2.3, p. 25. ISBN: 978-3527412143.

[9] A. Hansen, P. C. Hemmer, and S. Pradhan. *The Fiber Bundle Model. Modeling Failures in Materials*. 1st ed. Wiley VCH, 2015. Chap. 3.3.1, p. 39. ISBN: 978-3527412143.

[10] A. Hansen, P. C. Hemmer, and S. Pradhan. *The Fiber Bundle Model. Modeling Failures in Materials*. 1st ed. Wiley VCH, 2015. Chap. 2.3, pp. 21–26. ISBN: 978-3527412143.

[11] A. Hansen, P. C. Hemmer, and S. Pradhan. *The Fiber Bundle Model. Modeling Failures in Materials*. 1st ed. Wiley VCH, 2015. Chap. 3.3, pp. 46–48. ISBN: 978-3527412143.

[12] K. Rottmann. *Matematisk Formelsamling*. Spektrum forlag, 2010. Chap. VII, p. 105. ISBN: 978-82-7822-005-4.

[13] S. P. Timoshenko. *History of Strength of Materials. With a Brief Account of the History of Theory of Elasticity and Theory of Structures*. Dover Publications, Inc., 1983. Chap. V, p. 113. ISBN: 0-486-61187-6.

[14] P. C. Hemmer. *Kvantemekanikk*. 5th ed. Tapir Akademisk Forlag, 2005. Chap. 10, pp. 216–217. ISBN: 978-82-519-2028-5.

[15] C. Sanderson. *Armadillo: An Open Source C++ Linear Algebra Library for Fast Prototyping and Computationally Intensive Experiments*. Tech. rep. NICTA, 2010. URL: http://arma.sourceforge.net/armadillo_nicta_2010.pdf.

[16] G. H. Golub and C. F. Van Loan. *Matrix Computations*. 4th ed. The Johns Hopkins University Press, 2013. Chap. 11.3, pp. 625–637. ISBN: 978-1-4214-0794-4.

[17] G. H. Golub and C. F. Van Loan. *Matrix Computations*. 4th ed. The Johns Hopkins University Press, 2013. Chap. 11.2.7, pp. 619–620. ISBN: 978-1-4214-0794-4.

[18] G. H. Golub and C. F. Van Loan. *Matrix Computations*. 4th ed. The Johns Hopkins University Press, 2013. Chap. 11.6, pp. 670–680. ISBN: 978-1-4214-0794-4.

[19] G. H. Golub and C. F. Van Loan. *Matrix Computations*. 4th ed. The Johns Hopkins University Press, 2013. Chap. 11.3.7, pp. 634–635. ISBN: 978-1-4214-0794-4.

[20] G. H. Golub and C. F. Van Loan. *Matrix Computations*. 4th ed. The Johns Hopkins University Press, 2013. Chap. 11.3.9, pp. 636–637. ISBN: 978-1-4214-0794-4.

[21] J. Hoshen and R. Kopelman. "Percolation and cluster distribution. I. Cluster multiple labeling technique and critical concentration algorithm". In: *Phys. Rev. B* 14 (8 Oct. 1976), pp. 3438–3445. DOI: 10.1103/PhysRevB.14.3438. URL: http://link.aps.org/doi/10.1103/PhysRevB.14.3438.

[22] M. H.-S. Dahle. "Critical Behaviour of the Local Load Sharing Fiber Bundle Model". MA thesis. Norwegian University of Science and Technology, Jan. 2016.

[23] M. H.-S. Dahle. Private communication.

[24] A. Hansen, P. C. Hemmer, and S. Pradhan. *The Fiber Bundle Model. Modeling Failures in Materials*. 1st ed. Wiley VCH, 2015. Chap. 4.5.1, pp. 114–115. ISBN: 978-3527412143.

[25] A. Hansen, P. C. Hemmer, and S. Pradhan. *The Fiber Bundle Model. Modeling Failures in Materials*. 1st ed. Wiley VCH, 2015. Chap. 4.2.2, p. 103. ISBN: 978-3527412143.

[26] A. Stormo. "Brittle to Quasi-Brittle Transitions in the Soft Clamp Fiber Bundle Model". PhD thesis. Norwegian University of Science and Technology, Oct. 2013. ISBN: 978-82-471-4748-1.